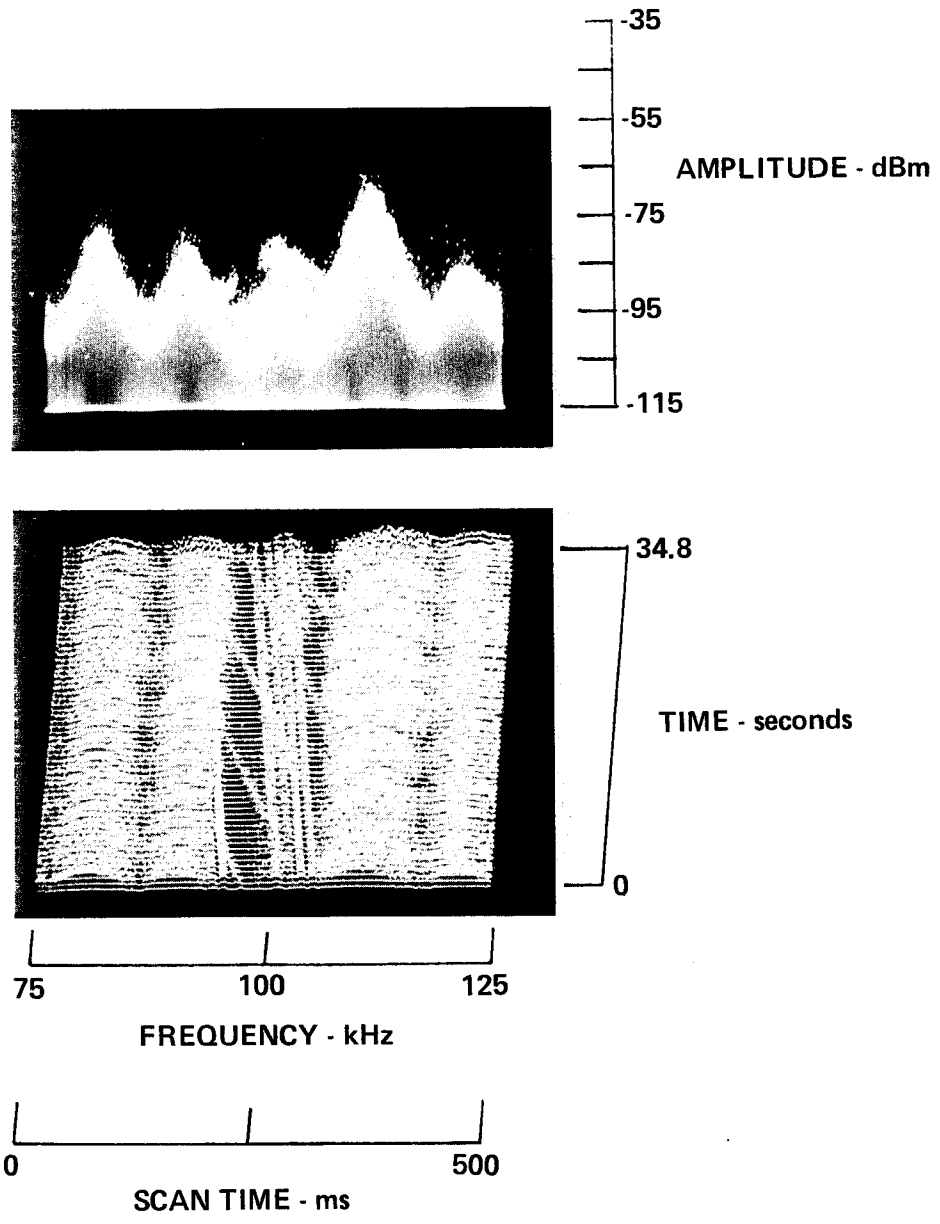


1-25-79, 0932, 110-048
HP140, Whip, F100, W50, IF3, ST 500, A -20/0/+15

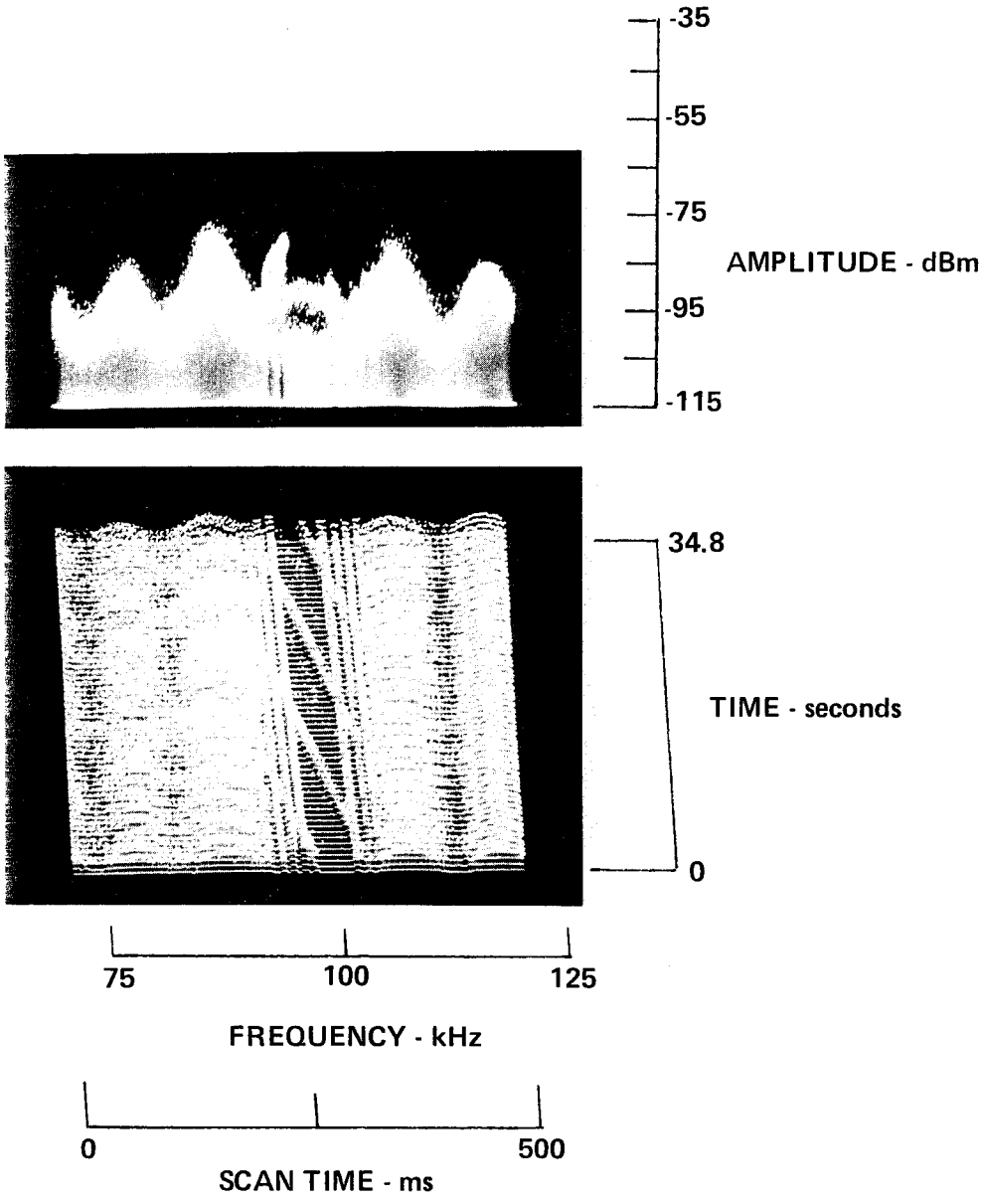


1-25-79, 0948, 110-049
HP140, Whip, F100, W50, IF3, ST 500, A -20/0/+15/NF

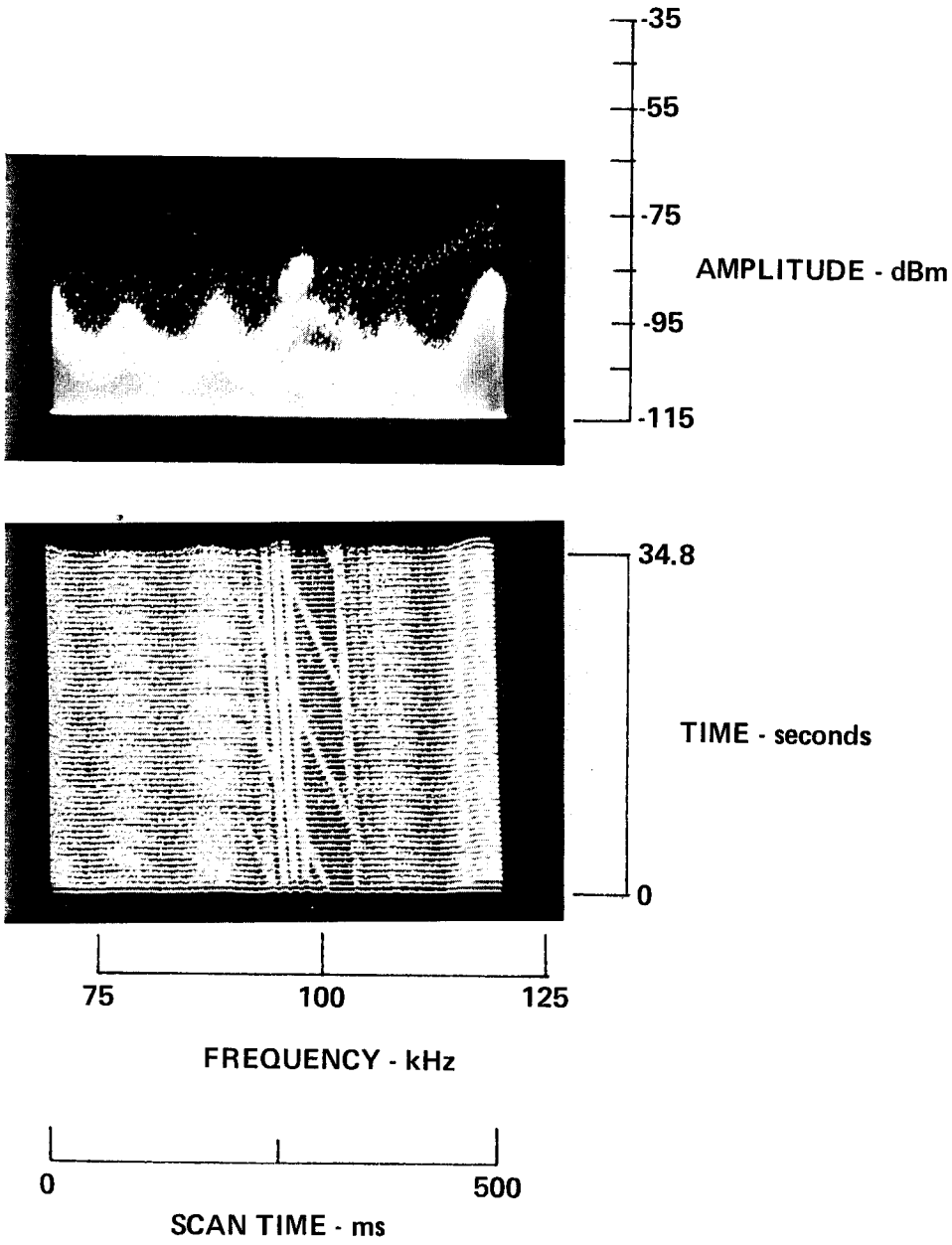


1-25-79, 0958, 110-050
HP140, Whip, F100, W50, IF3, ST 500, A -20/0/+15/NF

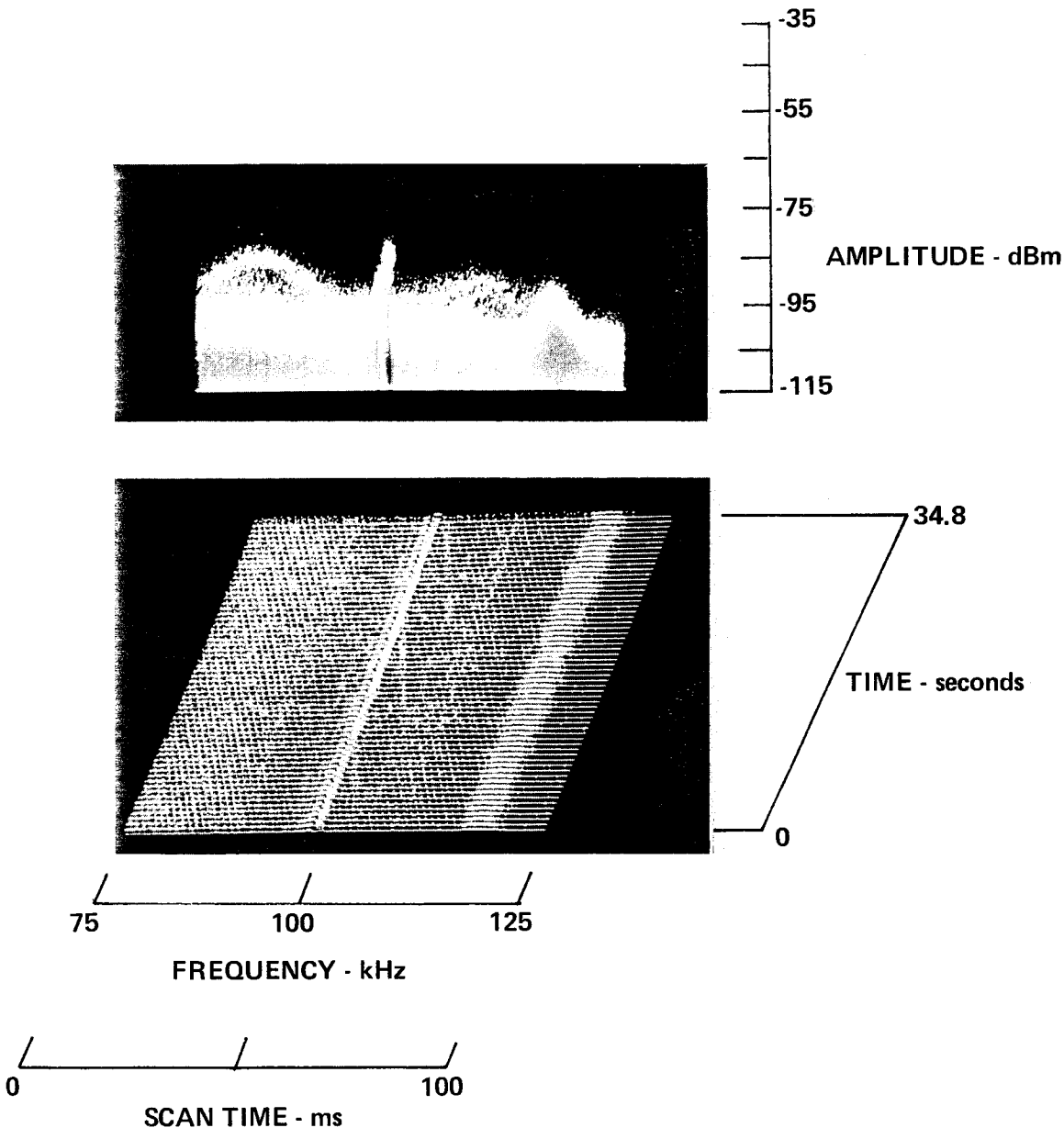


1-25-79, 1228, 104-051
HP140, Whip, F100, W50, IF3, ST 100, A -20/0/+15/NF

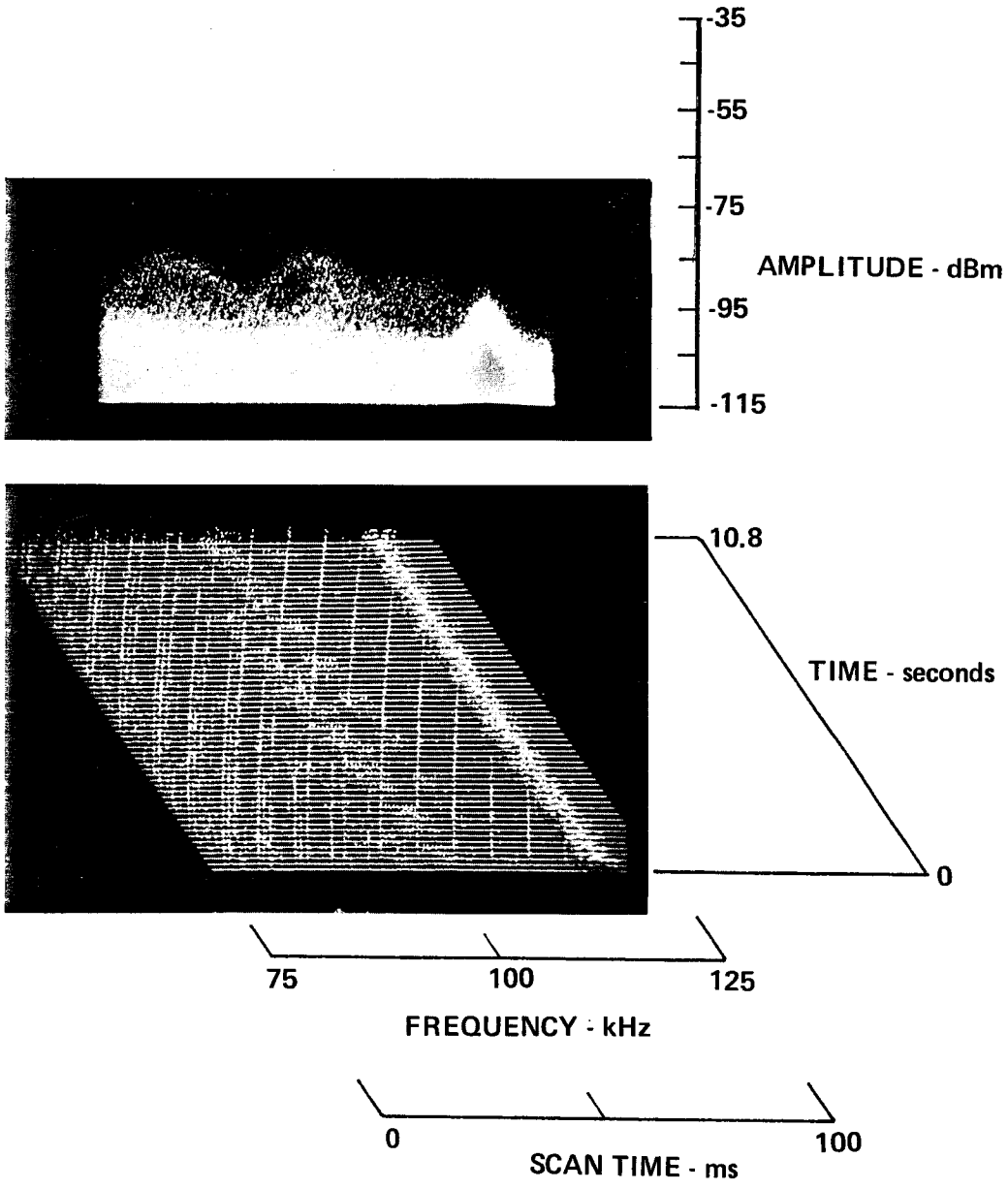


1-25-79, 1227, 104-051
HP140, Whip, F100, W50, IF3, ST 100, A -20/0/+15

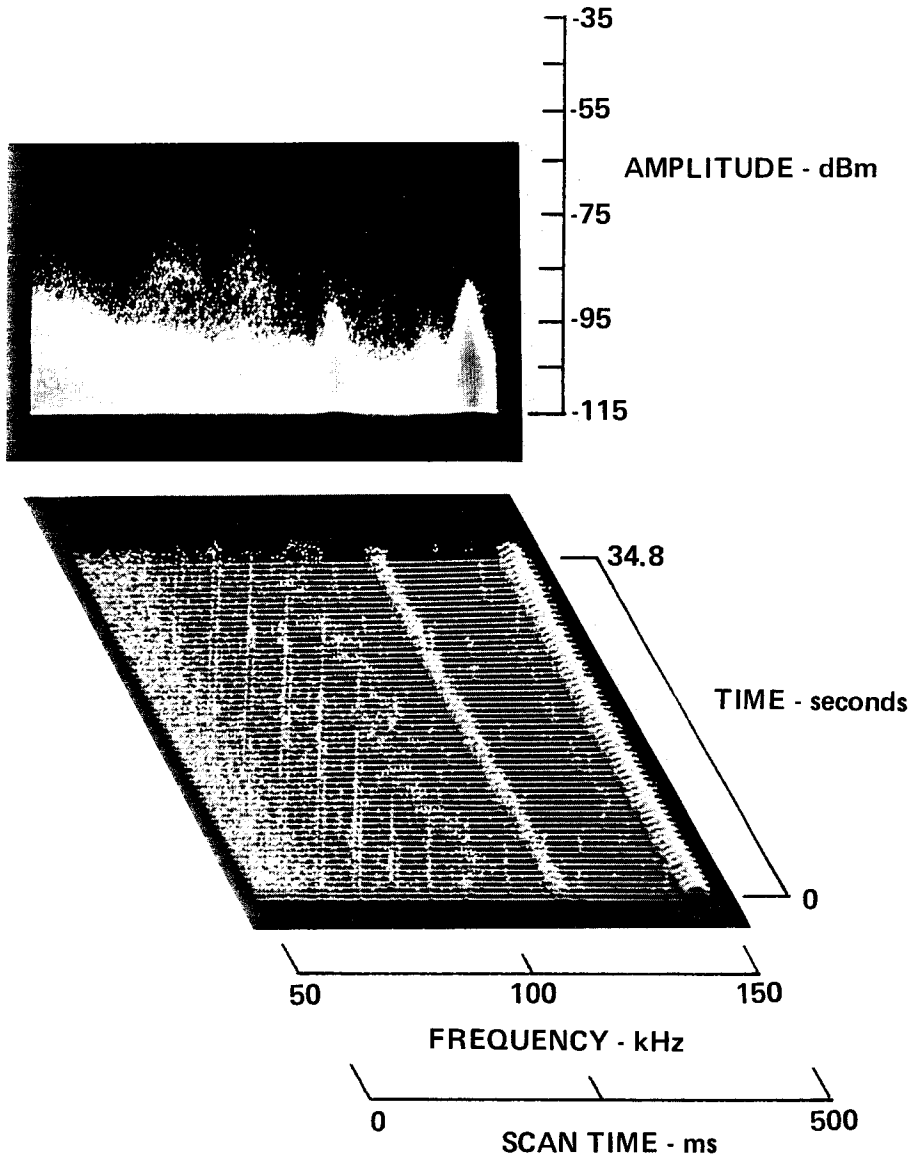


1-25-79, 1230, 104-051
HP140, Whip, F100, W100, IF3, ST 500, A -20/0/+15/NF

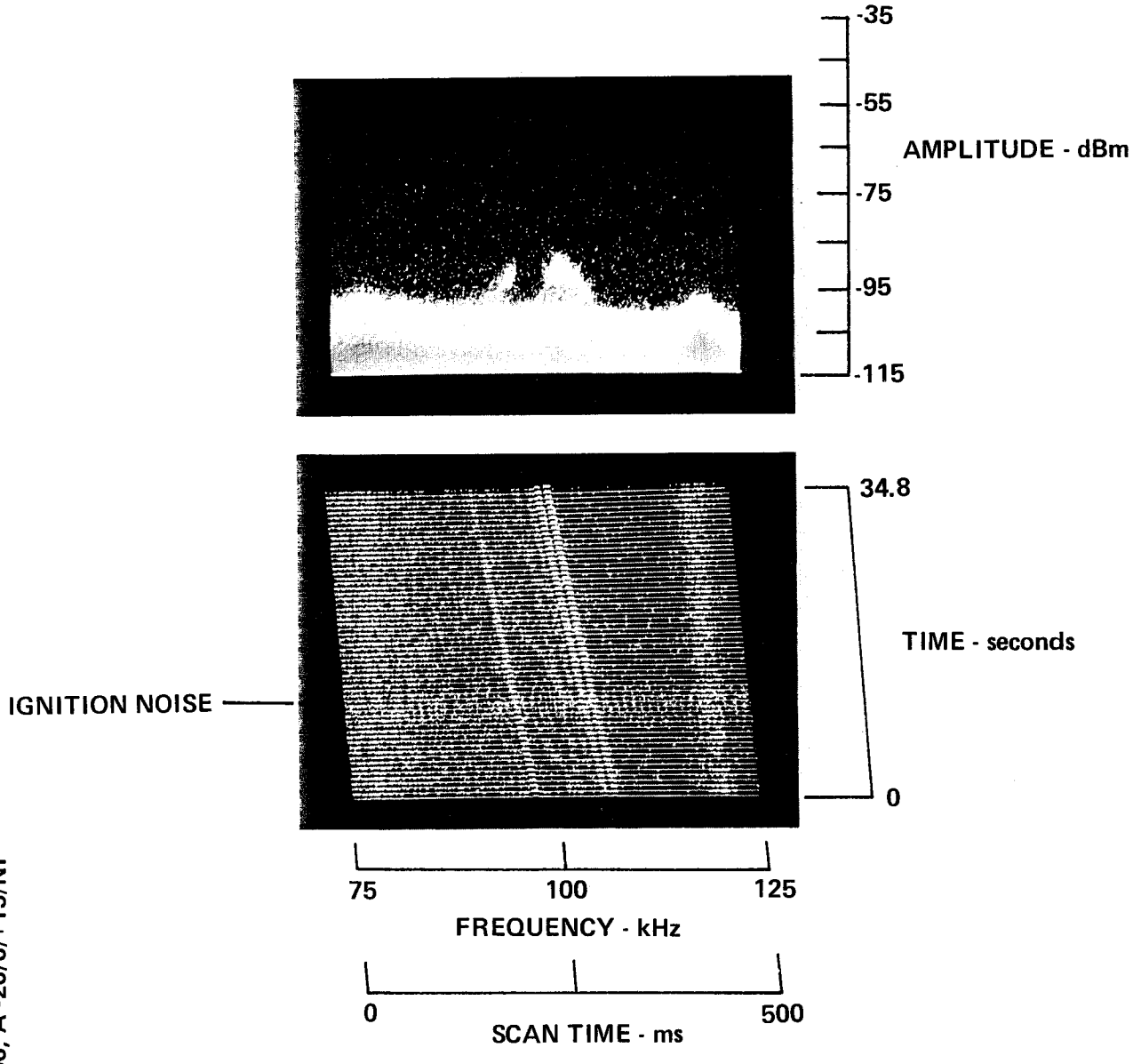


1-25-79, 1238, 104-052
HP140, Whip, F100, W50, IF3, ST 500, A -20/0/+15/NF

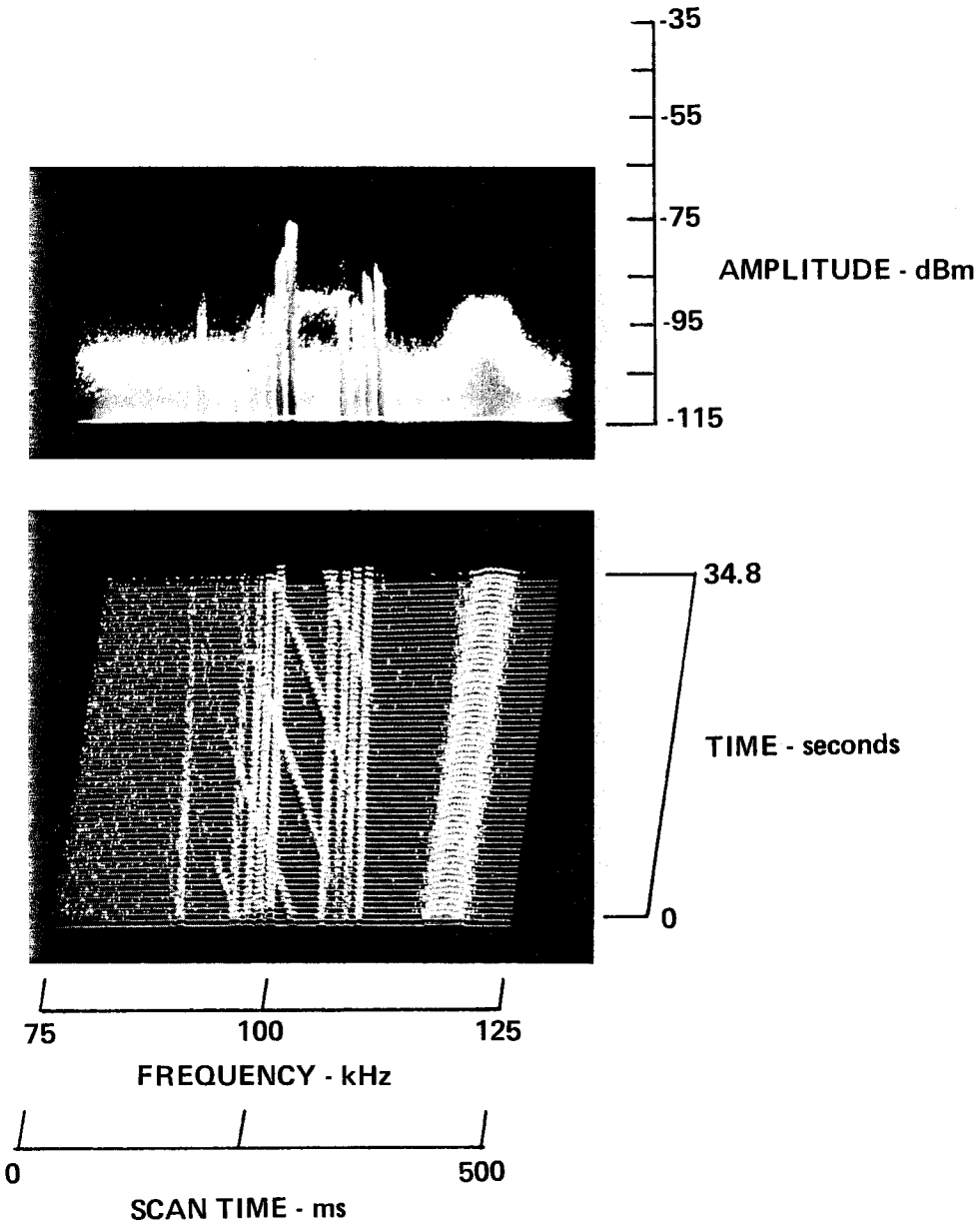


1-25-79, 1253, 104-053
HP140, Whip, F100, W50, IF3, ST 500, A -20/0/+15/NF

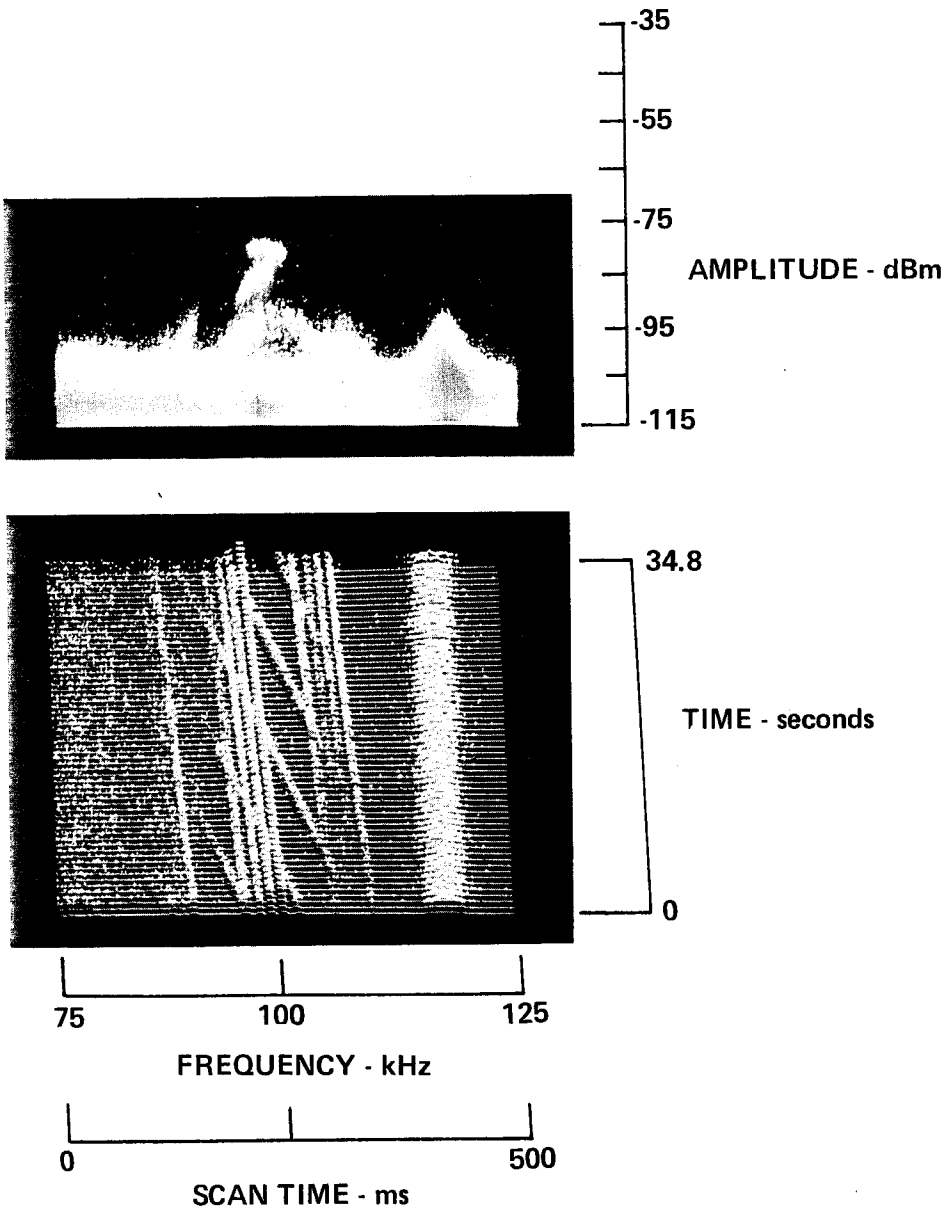


1-25-79, 1306, 104-054
HP140, Whip, F100, W50, IF3, ST 500, A -20/0/+15/NF

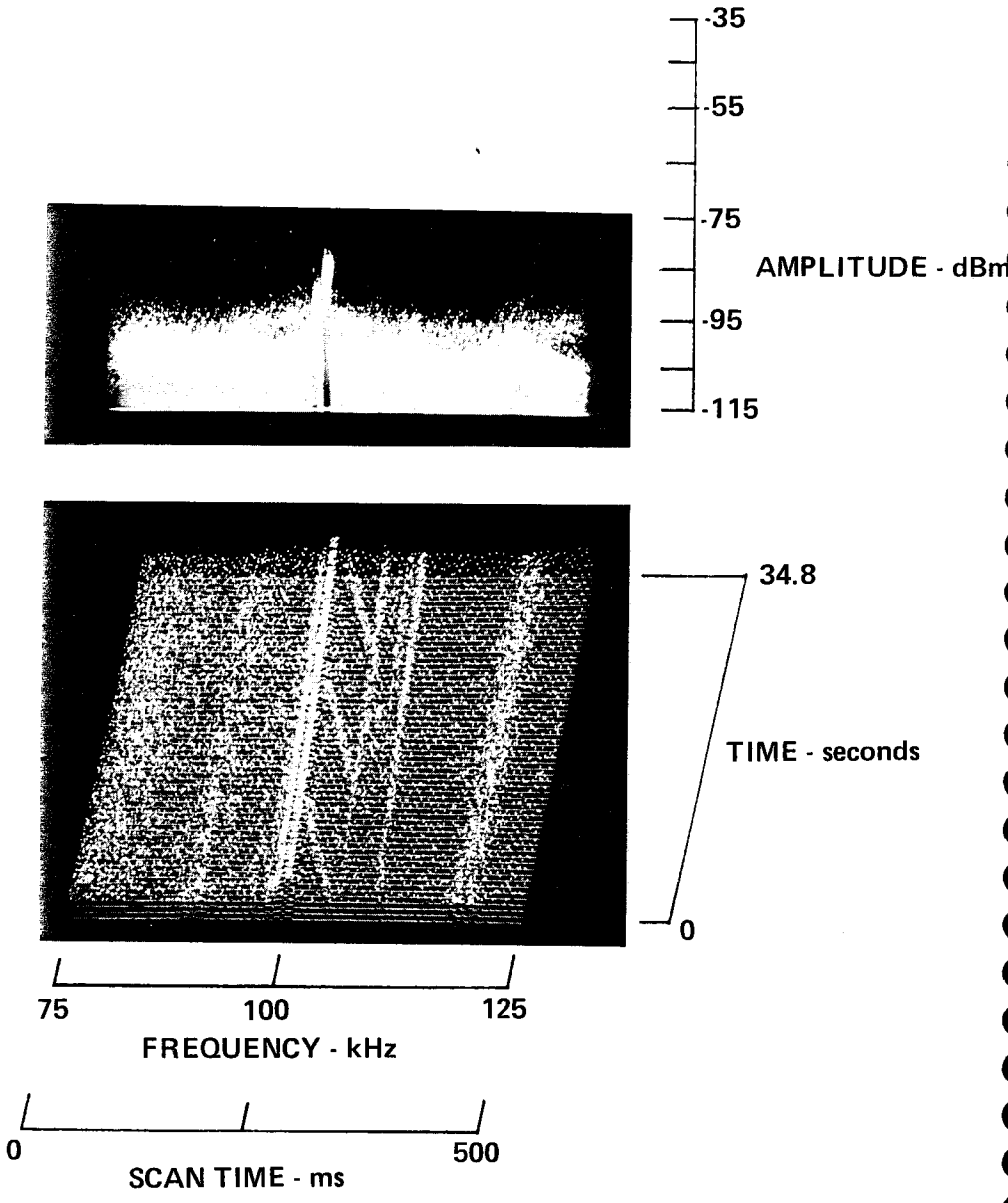


1-25-79, 1322, 104-055
HP140, Whip, F100, W50, IF3, ST 500, A -20/0/+15/NF

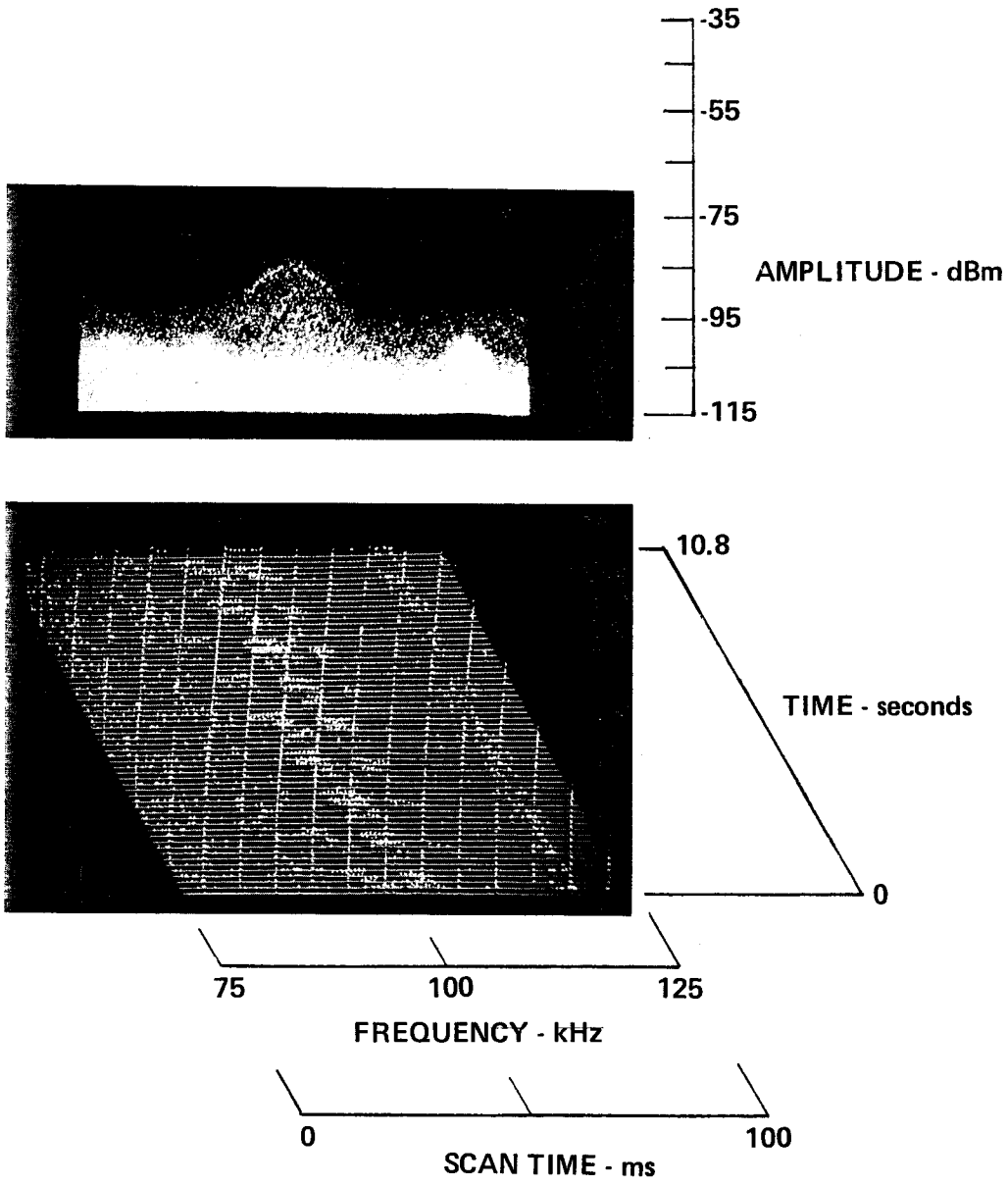


1-25-79, 1321, 104-055
HP140, Whip, F100, W50, IF3, ST 100, A -20/0/+15/NF

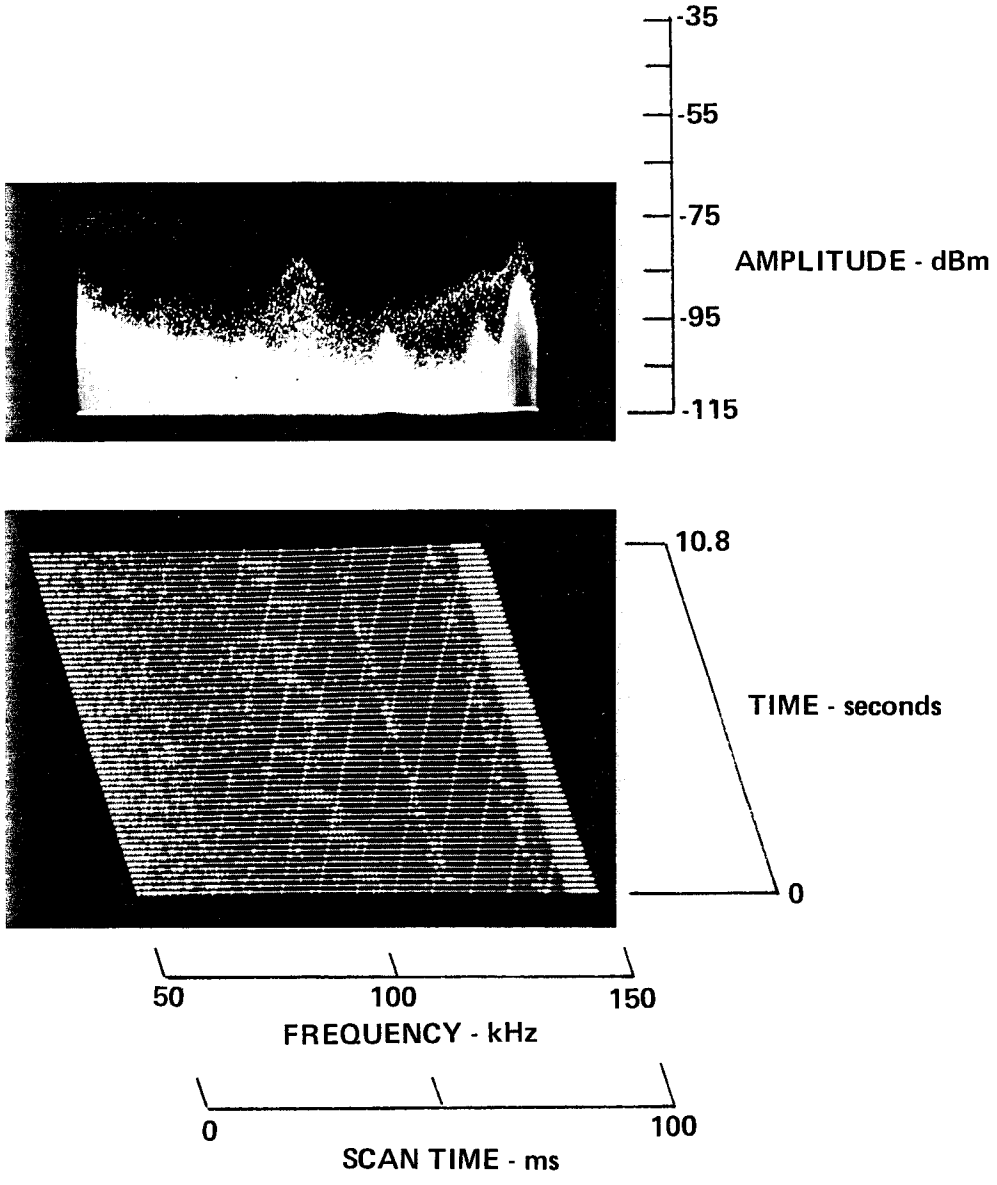


1-25-79, 1325, 104-055
HP140, Whip, F100, W100, IF3, ST100, A-20/0/+15/NF

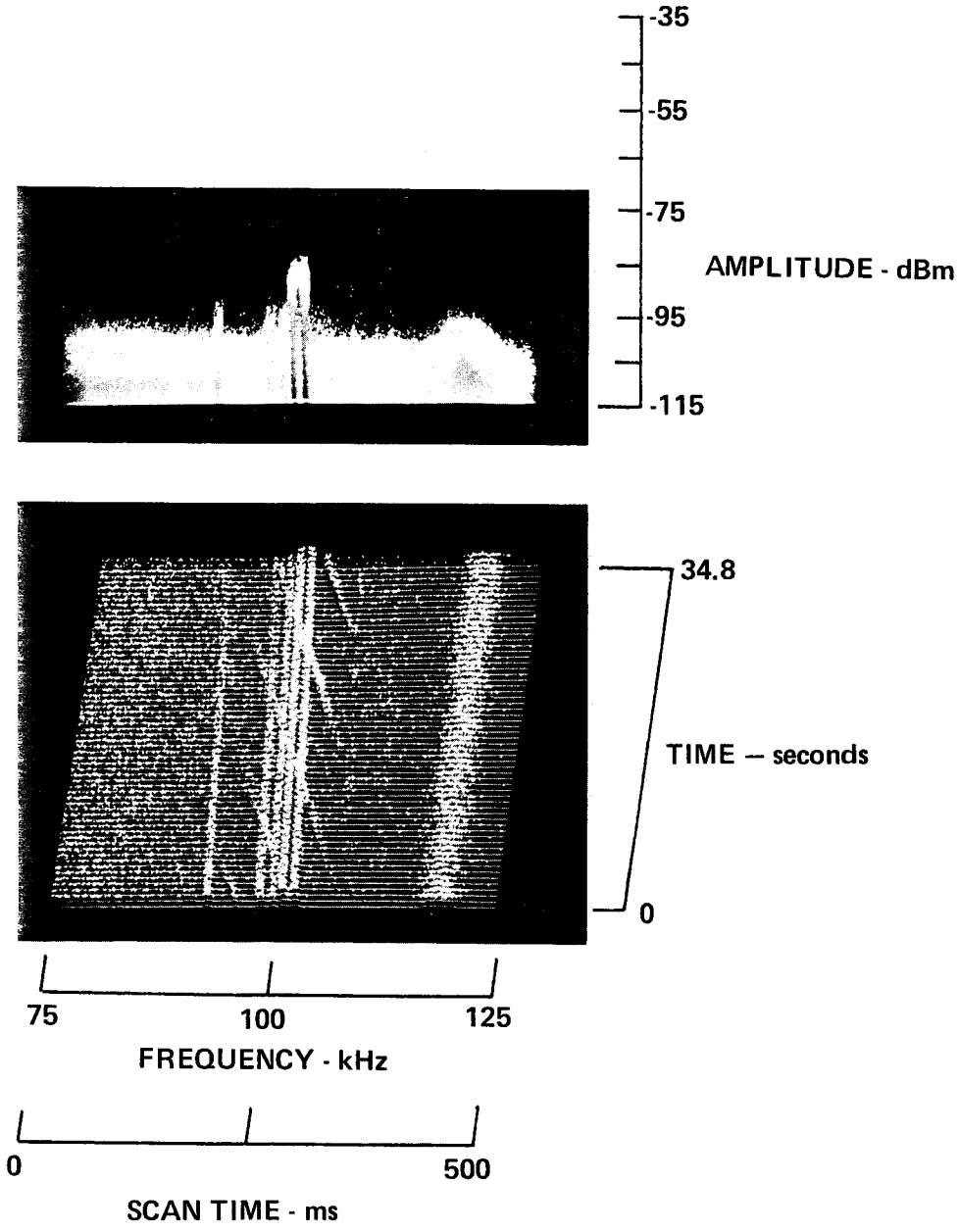


1-25-79, 1332, 104-056
HP140, Whip, F100, W50, IF3, ST 500, A -20/0/+15/NF

# APPENDIX B

## REPORT OF NEW TECHNOLOGY

The work performed under this contract during the collection and analysis of noise and interference data as reported herein has led to data on the types of interference expected to be encountered in the Loran-C band for the urban environment. This is the first quantified data of this type for the urban environment.

## REFERENCES


1. D.A. Feldman, "An Atmospheric Noise Model with Application to Low Frequency Navigation Systems," Ph.D. Thesis, Massachusetts Institute of Technology, June 1972.

2. P.G. Mauro and J.D. Gakis, "The Effects of Primary Power Transmission Lines on the Performance of Loran-C Receivers in Experimental Terrestrial Applications," Report No. DOT-TSC-RSPA-79-8, July 1979.

3. R.A. Shepard, J.W. Engles, and G.H. Hagn, "Automobile Ignition Noise and the Super Noisy Vehicle," EMC Symposium Record, IEEE 76-CH-1104-9-EMC, pp. 403-412, 1976.

4. G.H. Hagn, "Definitions and Fundamentals of Electromagnetic Noise, Interference, and Compatibility," NATO/AGARD Meeting on Electromagnetic Noise, Interference, and Compatibility, October 21-25, 1974, Paris, France.

5. "Manual of Regulations and Procedures for Radio Frequency Management," Office of Telecommunications Policy, Executive Office of the President.

6. "World Distribution and Characteristics of Atmospheric Radio Noise," CCIR Report 332, ITU, Geneva, Switzerland, 1964.

7. R.J. Matheson, "Instrumentation Problems Encountered Making Man-Made Electromagnetic Noise Measurements for Predicting Communications Performance," IEEE Trans. on Electromagnetic Compatibility, Vol. EMC-12, No. 4, November 1970.

8. A.D. Spaulding and R.T. Disney, "Man-Made Radio Noise, Part I: Estimates for Business, Residential, and Rural Areas," OT REport 74-38, Office of Telecommunications, U.S. Department of Commerce, June 1974.

9. A.D. Spaulding, "Man-Made Radio Noise: The Problem and Recommended Steps Toward Solution," OT Report 76-85, Office of Telecommunications, U.S. Department of Commerce, April 1976.

10. E.N. Skomal, Man-Made Radio Noise, Van Nostrand Reinhold Co., 1978.

11. D.A. Feldman, "An Atmospheric Noise Model with Application to Low Frequency Navigation Systems," Ph.D. Thesis, Massachusetts Institute of Technology, June 1972.

12. E.N. Skomal, "Results of an AM Broadcast AVL Experiment," IEEE Transactions on Vehicular Technology, Vol. VT-26, No. 1, February 1977.

# BIBLIOGRAPHY


L.O. Barthold, et al., "Transmission Line Reference Book, 115-138 KV Compact Line Design," Electric Power Research Institute, Palo Alto, California, 1978.

R.B. Churchill, "Modeling the Relative Amplitude Probability Distribution of Power Line Noise," ESD-TR-75-019, DOD Electromagnetic Compatibility Analysis Center, Annapolis, Maryland, October 1975.

R.A. Shepard and J.C. Gaddie, "Measurement of the APD and the Degradation Caused by Power Line Noise at HF," Final Report, Contract N00039-74-C-0077, Stanford Research Institute, Menlo Park, California, April 1976.

Course Text, IEEE Tutorial Course, "The Location, Correction, and Prevention of RI and TVI Sources from Overhead Power Lines," IEEE, New York, New York, 1975.

M.S. Gupta, Electrical Noise Fundamentals and Sources, IEEE Press, New York, New York, 1977.

R. Caldicott, et al., "Model Study of Electric Field Effects in Sub-Stations," EPRI EL-632, prepared by Ohio State University for the Electric Power Research Institute, Palo Alto, California, January 1978.

L.E. Zaffanella and D.W. Deno, "Electrostatic and Electromagnetic Effects of Ultrahigh-Voltage Transmission Lines," EPRI EL-802, prepared by General Electric Company for the Electric Power Research Institute, Palo Alto, California, June 1978.

H.N. Shaver, V.E. Hatfield, and G.H. Hagn, "Man-Made Radio Noise Parameter Identification Task," Final Report, Contract N00039-71-A0223, Stanford Research Institute, Menlo Park, California, May 1972.

R.A. Shepard, J.C. Gaddie, V.E. Hatfield, and G.H. Hagn, "Measurements of Automobile Ingition Noise at HF," Final Report, Contract N00039-71-A-0223, Stanford Research Institute, Menlo Park, California, February 1973.

Special Issue on Spectrum Management, IEEE Trans. on Electromagnetic Compatibility, Vol. EMC-19, No. 19, August 1977.

W.R. Lauber, "Amplitude Probability Distribution Measurements of the Apple Grove 775 KV Project, " IEEE Trans. on Power Apparatus and Systems, Vol. PAS-95, No. 4, July/August 1976.

A.D. Watt and E.L. Maxwell, "Measured Statistical Characteristics of VLF Atmospheric Radio Noise," Proc. IRE, Vol. 45, pp. 55-62, January 1957.

R.A. Shepard, "Measurements of Amplitude Probability Distributions and Power of Automobile Ignition Noise at HF," IEEE Trans. on Vehicular Technology, Vol. VT-23, No. 3, August 1974.

SRI International

January 1981

Technical Memorandum

# Electric and Magnetic Fields Emanating From a Utility Distribution Line

By:

Wilbur R. Vincent
Robert Bollen
John Meloy

333 Ravenswood Ave. • Menlo Park, California 94025
(415) 326-6200 • Cable: SRI INTL MPK • TWX: 910-373-1246

## ABSTRACT

Radio noise conducted along and electromagnetic fields associated with a selected "noisy" suburban-area distribution line were investigated. The spatial, temporal, and spectral properties of the noise were emphasized. Because the measurements were made directly under the power line, both electric- and magnetic-field sensors were used to describe the inductive or quasi-static region fields associated with the overhead line. Magnetic-field data were translated into noise current, and electric-field data were translated into noise voltage on the overhead wires. Effective impedance magnitude of the noise was determined over a broad band of frequencies.

# I INTRODUCTION

A large number of technical papers describing the radio and electrical noise associated with electric utility power lines have appeared in the literature. Many of these papers have presented excellent statistical data on power-line noise[1-5] and on specific properties of power-line noise.[6-8] Yet, some aspects of power-line-associated radio noise are confusing and poorly understood by engineers and technicians who encounter the effects of such noise on operational communications and navigation systems.

To better understand the primary properties of power-line noise, a suburban utility distribution line that had an established reputation as a "noisy" line was investigated. E- and B-field sensors were used to measure the electric and magnetic fields of noise associated with the line. Determining the magnitude of each field was emphasized as well as temporal and spectral properties over a broad band of frequencies. The results obtained from the investigation are presented.

## II INSTRUMENTATION

The instrumentation van used for the measurements was similar to that used in a number of previous investigations on power-line noise.[9,10] Figure 1 is a block diagram showing the major components of the instrumentation. The data described in this paper are from the scanning receiver portion of the overall instrumentation package. The channelized receiver collected supporting data. The scanning receiver was a Hewlett Packard Series 140 Spectrum Analyzer interfaced with a Develco Model 7200B 3-Axis Display. The instrumentation produced a real-time visual display of all signals and noise within the frequency scan range of the spectrum analyzer. The scan time of the spectrum analyzer was always set for a longer period than several periods of the 60-Hz line waveform so that several successive power-line noise impulses could be received during each scan. This procedure produced an unambiguous view of impulses received during 60 successive analyzer scans. The data contained finely scaled temporal information and relatively coarsely scaled spectral data.

The B-field sensor was a Faraday-shielded ferrite-core loopstick designed for uniform response to incident magnetic fields over the 50-Hz to 250-kHz band of frequencies. Other B-field sensors were available for higher frequencies, but they were not employed during the reported measurements. The E-field sensor was a one-meter vertical rod located on the roof of the instrumentation van. The preamplifier gain-versus-frequency curve was shaped to provide a uniform response to incident E-fields over the 50-Hz to 250-kHz band of frequencies. Equal B- and E-field response was obtained by adjusting the gain of the E-field amplifier when receiving known far-field signals. This procedure permitted B-field amplitude to be calibrated in Tesla (T) or Weber/meter$^2$ (Web/m$^2$), and E-field amplitude to be calibrated in V/m over the entire band of frequencies under observation.

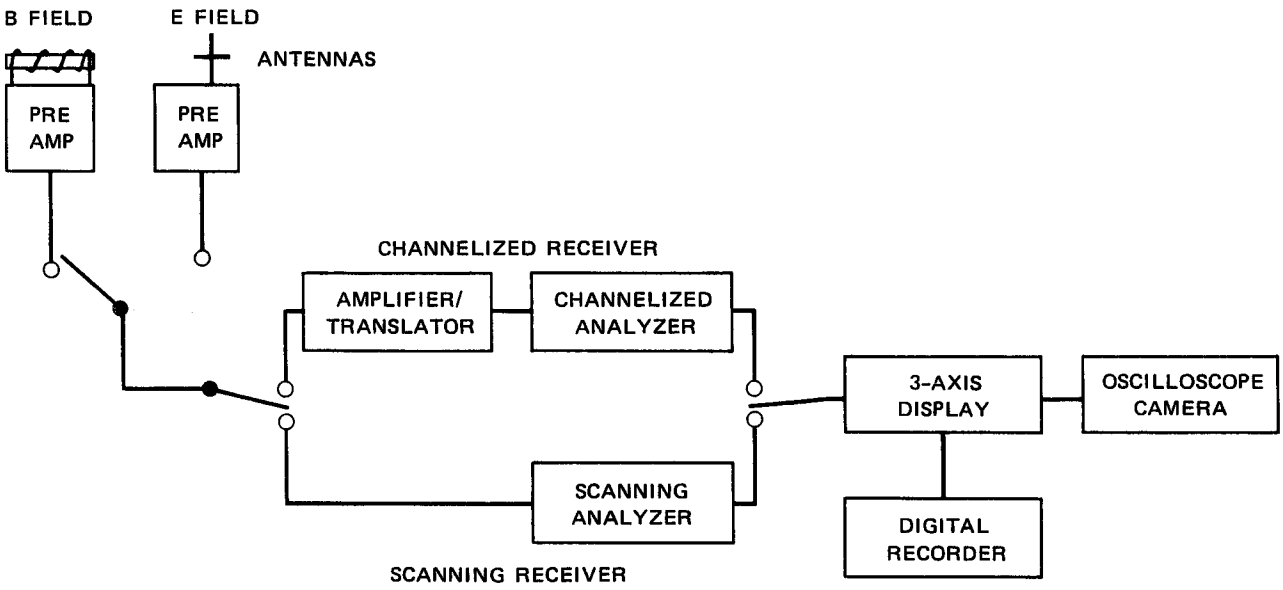


FIGURE 1 BLOCK DIAGRAM OF INSTRUMENTATION

Each 3-axis view of noise data contains a listing of pertinent site and instrumentation parameters used for the view. These parameters are identified as follows:

- Date and local time
- Site location and line identification
- Center frequency
- Frequency scan width
- IF filter bandwidth
- Scan time
- Preamplifier gain, analyzer RF gain, analyzer IF gain.

## III MEASUREMENTS

The distribution line selected for measurements was a 12-kV single-phase two-wire overhead line located along a short dead-end street in a medium size California residential city. The street was located in the center of a large residential area and was about two miles from a small-town business area. Small manufacturing establishments were located four miles or more from the selected line. The line served five residential customers from two pole-mounted, single-phase step-down transformers. Figure 2 is a map of the physical layout and measurement geometry.

The noise on the line selected has caused faulty operation of experimental radio-navigational systems, noise on AM automobile radios, and undesired operation of the squelch of mobile VHF radios. An inspection of the line revealed no obviously faulty hardware or common sources of power-line noise.

Noise over the 0- to 200-kHz band of frequencies was measured midway along the line (Site 1) at midday and is shown in Figure 3. The 3-axis view shows an amplitude-compressed view of all signals and noise within the frequency band: the top half of the view shows E-field signals and the bottom half of the view shows B-field signals. The constant frequency signals in the 3-axis view were from distant VLF and LF transmitters. The sharp slanting lines were from E- and B-field impulses that emanated from the overhead line. These impulses had a period of 8.33 ms, indicating that they were synchronized with both the positive and negative portions of the 60-Hz-line-voltage waveform. The E-field data shown in the upper half of the 3-axis view were portrayed in an amplitude-versus-frequency format in the upper photograph. The B-field data shown in the lower half of the 3-axis view were portrayed in a similar manner in the center photograph. The amplitude of signals and background noise can be

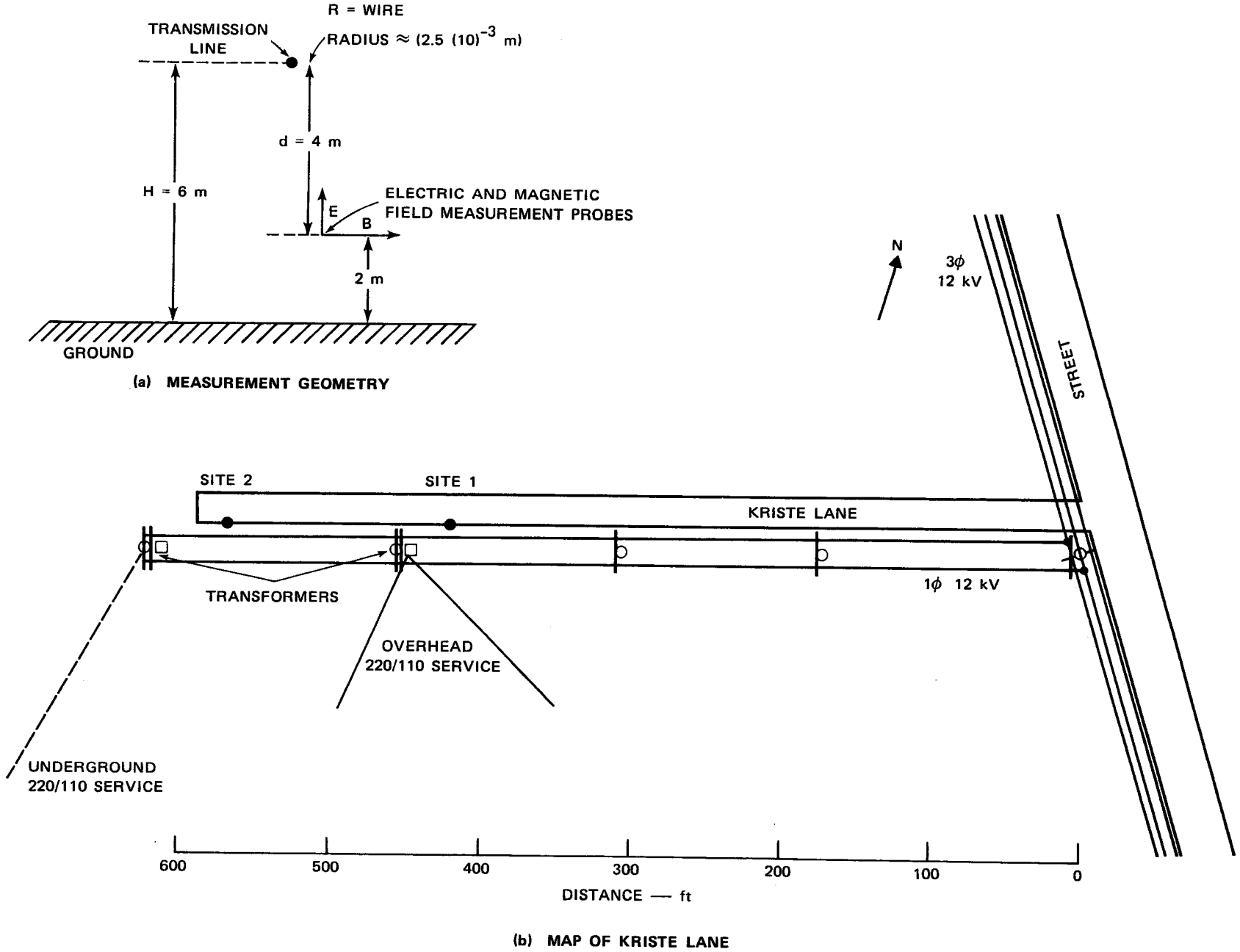


FIGURE 2 MAP OF FIELD SITE AND MEASUREMENT GEOMETRY

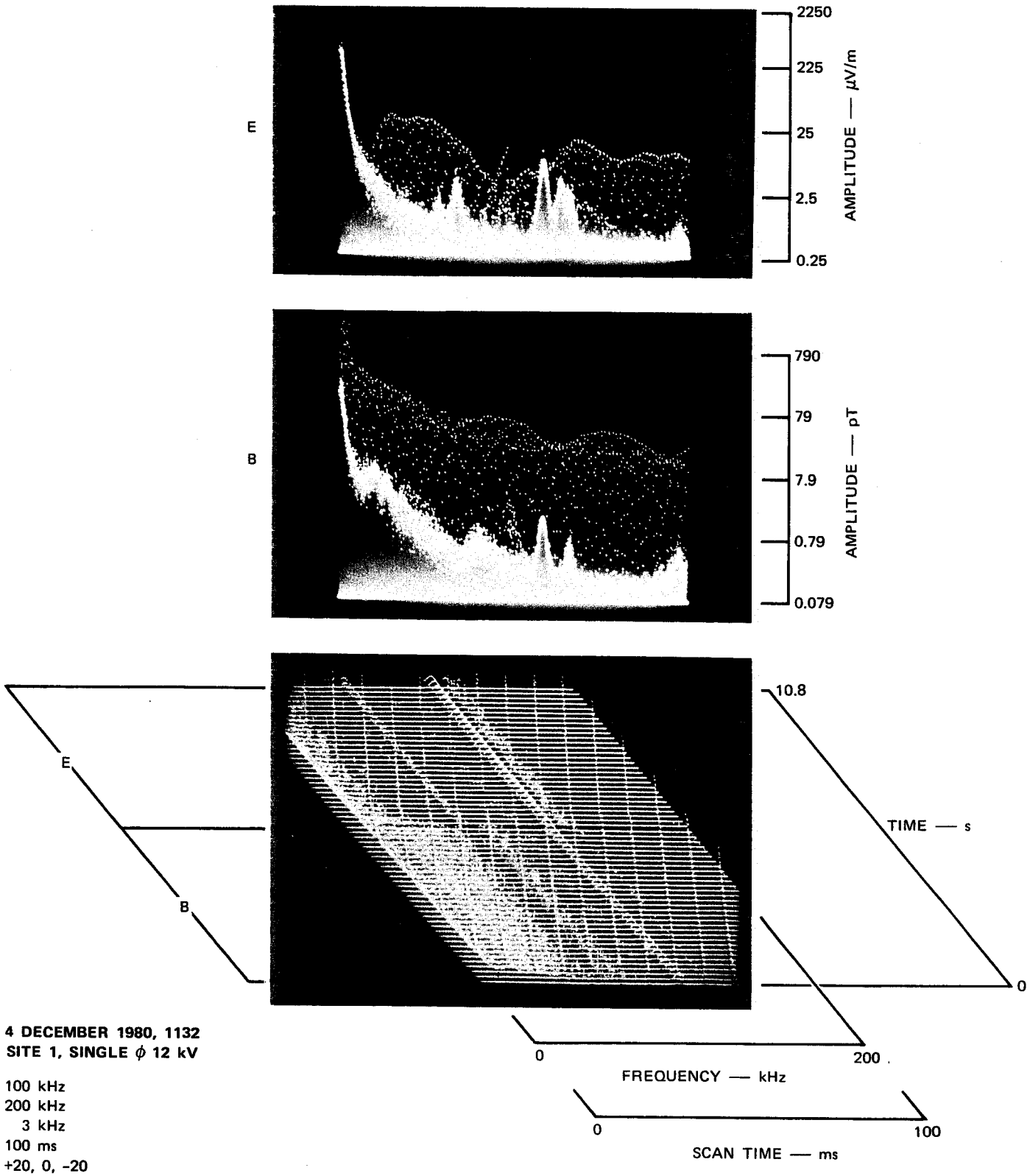


FIGURE 3 E- AND B-FIELD NOISE AT SITE 1 — MIDDAY

seen as well as the high-level impulse noise. The field strength of signals and noise are shown in V/m or T.

Although the strength of CW signals can be read directly from the amplitude scale of the 3-axis views, the impulses did not rise to full amplitude because of IF bandwidth limitations. An empirically determined factor of 12 dB must be added to all impulse amplitudes to obtain the true peak amplitude.

The amplitude of the E-field impulses below 20 kHz is low. The impulses rise in amplitude and reach a broad peak between 30 and about 55 kHz. A null was found near 100 kHz followed by a second increase to a near-constant level from 160 kHz to the upper limit of the measurement at 200 kHz. The B-field maximum amplitude occurred at very low frequencies and was followed by a slow decline in amplitude across the observed band of frequencies. The amplitude peaks and nulls in the B-field data did not correspond to peaks and nulls in the E-field data. The E- and B-field sensors were in the overhead wires' inductive field where the E-field data are associated with line-to-ground noise voltage, and the B-field data are associated with the noise current that flowed along the line.

## IV CALCULATION OF LINE-NOISE PARAMETERS

At a distance of four meters from the wire [Figure 2(a)], the measurements were in the inductive or quasi-static field over the entire 50-Hz to 200-kHz frequency range. For instance, at the high end of the frequency band (200 kHz), the ratio of wavelength to distance (d) was almost 400. With the measurement probes directly under the outer wire of the line, the dominant magnetic-field vector, $\vec{B}$, would be parallel to the ground and perpendicular to the wire [Figure 2(a)], and the dominant electric-field vector, $\vec{E}$, would be vertical with respect to the ground.

The impulsive current and voltage in the overhead wire can be estimated if the approximations are used that the ground under the line has either (1) infinite or (2) zero conductance. The former approximation is applicable to power lines over swamp or marshy areas and the latter is applicable in desert areas or in areas of permafrost.

The relationship between measured magnetic-field strength and impulsive current in the overhead wire in free space or over a zero conductance ground plane is:

$$I = \frac{2\pi\ Bd}{\mu_o} \tag{1}$$

B = magnetic-field strength (T)

d = distance from the sensor to the line (m)

$\mu_o$ = permeability of free space ($4\pi \times 10^{-7}$)

I = current (A)

The effective line impedance at noise frequencies, $Z_L$, is:

$$|Z_L| \approx \frac{|E|}{|H|} \approx \frac{\mu_o |E|}{|B|} \quad . \tag{2}$$

The impedance magnitude as a function of the frequency for measurements obtained at Site 1 are shown in Figure 4. Distinct resonance peaks were found at 52, 125, and 175 kHz. Resonance nulls were found at 90 and 150 kHz and the average value of impedance increased with increasing frequency.

If we take the other approach and assume the wire was over a perfect ground plane, the equation for current in the line is:

$$I = \frac{\pi B\, d(2h - d)}{\mu_o} \tag{3}$$

h = height (in meters) of conductor over ground.

Equation (3) is only valid for measurements directly under the line. Expressions for arbitrary geometry are given by Pullen.[11]

A similar equation[12] for electric field is:

$$E = \frac{\rho_\ell}{2\pi\epsilon} \frac{2h}{d(2h - d)} \tag{4}$$

$\epsilon$ = permittivity of free space

$\rho_\ell$ = charge per unit length (coul/m)

The expression for line voltage, $V_L$, for a finite conductor over a perfect ground plane is:

$$V_L = \frac{\rho_\ell}{2\pi\epsilon} \ln \left(\frac{2h}{R}\right) \tag{5}$$

R = conductor radius (in meters) [assumed to be 2.5 $(10^{-3})$ m].

If we substitute Eq. (4) into Eq. (5), then

$$V_L = \frac{Ed\ (2h - d)}{2h} \ln \left(\frac{2h}{R}\right) \quad . \tag{6}$$

The calculated values for line current voltage and impedance are compared in Table 1 for the two assumptions considered. The calculated values from the equations applicable to each assumption are in close agreement.

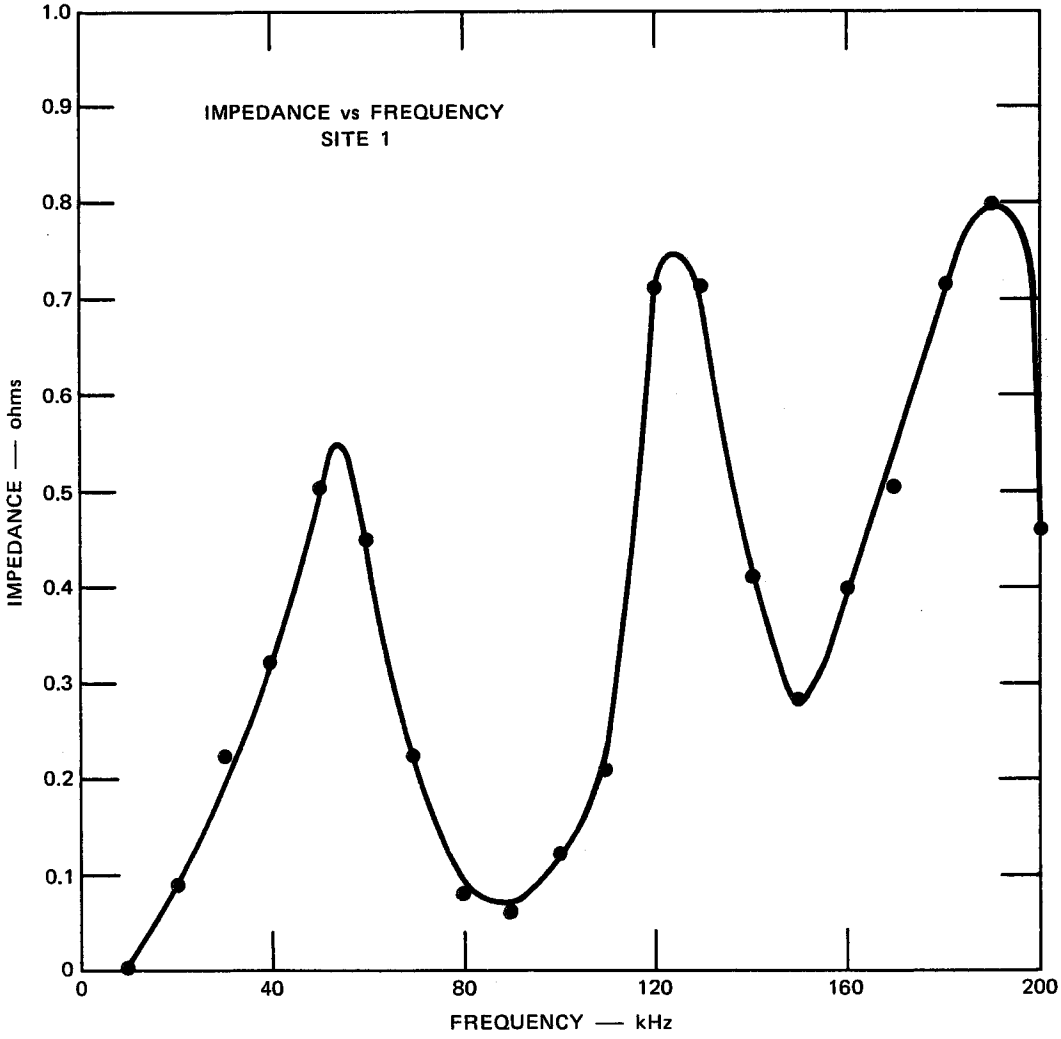


FIGURE 4 IMPEDANCE MAGNITUDE AS A FUNCTION OF FREQUENCY AT SITE 1

Table 1

CALCULATED VALUES OF NOISE VOLTAGE AND CURRENT
ON POWER LINE AT SELECTED FREQUENCIES

| Frequency (kHz) | Line in Free Space | | | Line Over Perfectly Conducting Ground Plane | | |
|---|---|---|---|---|---|---|
| | Noise Current (mA) | Noise Voltage (mV) | Impedance $\Omega(10^{-2})$ | Noise Current (mA) | Noise Voltage (mV) | Impedance $\Omega(10^{-2})$ |
| 10 | 35.4 | 0.3 | 0.8 | 23.6 | 0.3 | 1.1 |
| 50 | 6.3 | 3.2 | 50.2 | 4.2 | 2.9 | 68.1 |
| 100 | 4.5 | 0.6 | 12.7 | 3.0 | 0.5 | 17.1 |
| 200 | 2.0 | 0.9 | 45.1 | 1.3 | 0.8 | 60.8 |

## V OTHER MEASUREMENTS

Measurements were also made near the west end of the short street at a location about 150 ft west of the previous site. Somewhat different E- and B-field results were obtained at Site 2 as shown in Figure 5. At this location sharp nulls were found in the B field near 25 and 75 kHz, and the B field was generally lower in amplitude than at Site 1. The general shape for both sites of the E-field versus frequency data is similar.

Impedance as a function of frequency at the second location is shown in Figure 6. A small resonance peak was found at about 20 kHz along with larger peaks at 130 and 170 kHz. The impedance data were considerably different from that obtained at the previous location. The very large difference in impedance data from two locations on the same overhead line only 150 ft apart was surprising, and the data suggest that the various transformers, house feeders, transition from overhead to underground, and other line parameters involved represent complex circuits at the noise frequencies examined.

Another set of measurements were made at Site 1 during the early evening hours, and a somewhat different set of impulses were noted from the overhead line. Figure 7 shows the 3-axis view of temporal structure and the B- and E-field strength as a function of frequency. The E-field level was quite low; the B-field was of modest strength; and the E- and B-field impulses were spaced 8.3 ms apart. Careful inspection of the 3-axis view of Figure 7 shows a change in time displacement at the E- to B-field border, which implies that the E-field impulses originated from one source, and the B-field impulses originated from a second source whose line-synchronous firing time was slightly ahead of the E-field source in phase. Impedance values from such data would be meaningless. The example shows a key advantage of the high time-domain resolution of the instrumentation used to make the measurements. A standard noise

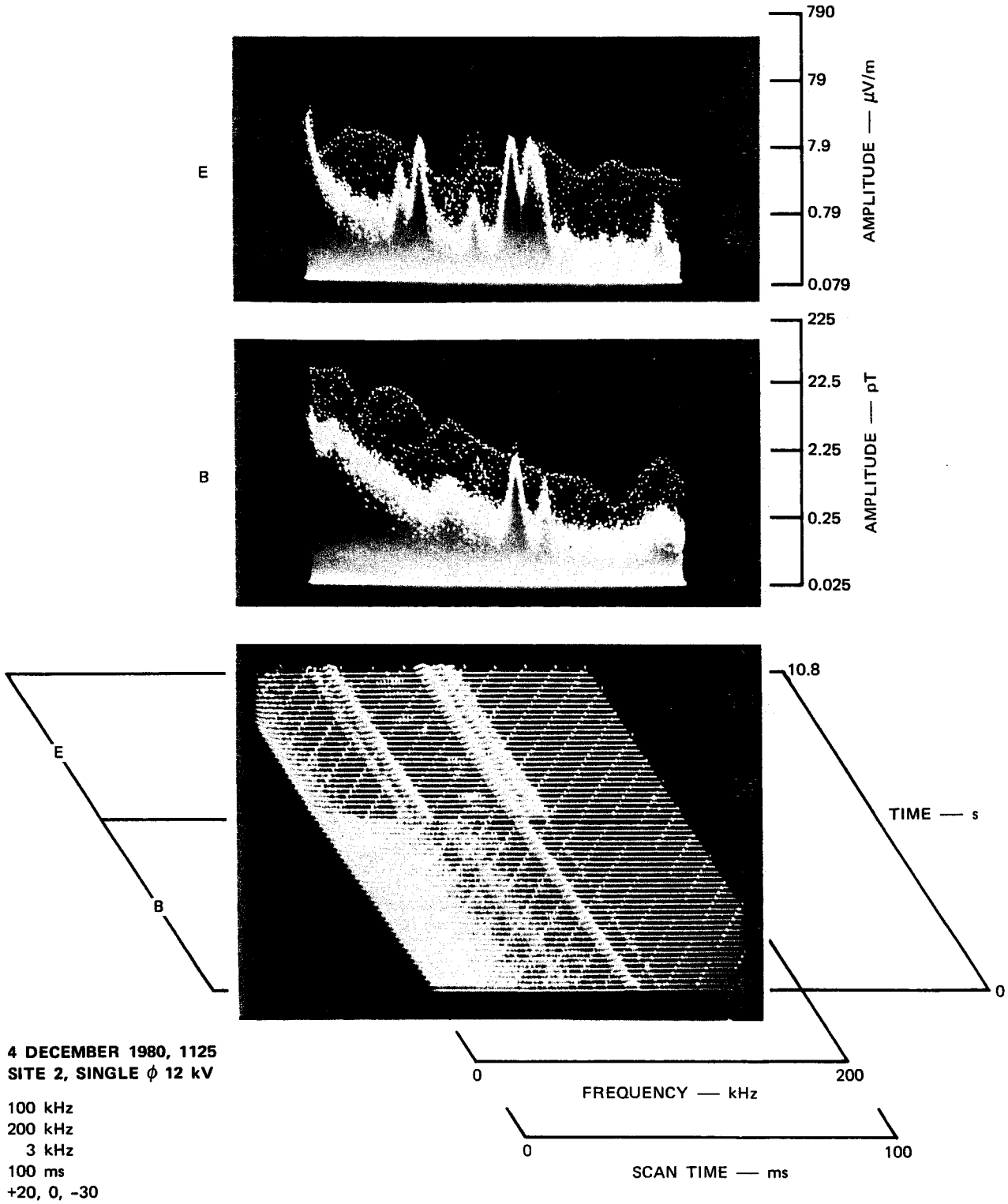


FIGURE 5 E- AND B-FIELD NOISE AT SITE 2

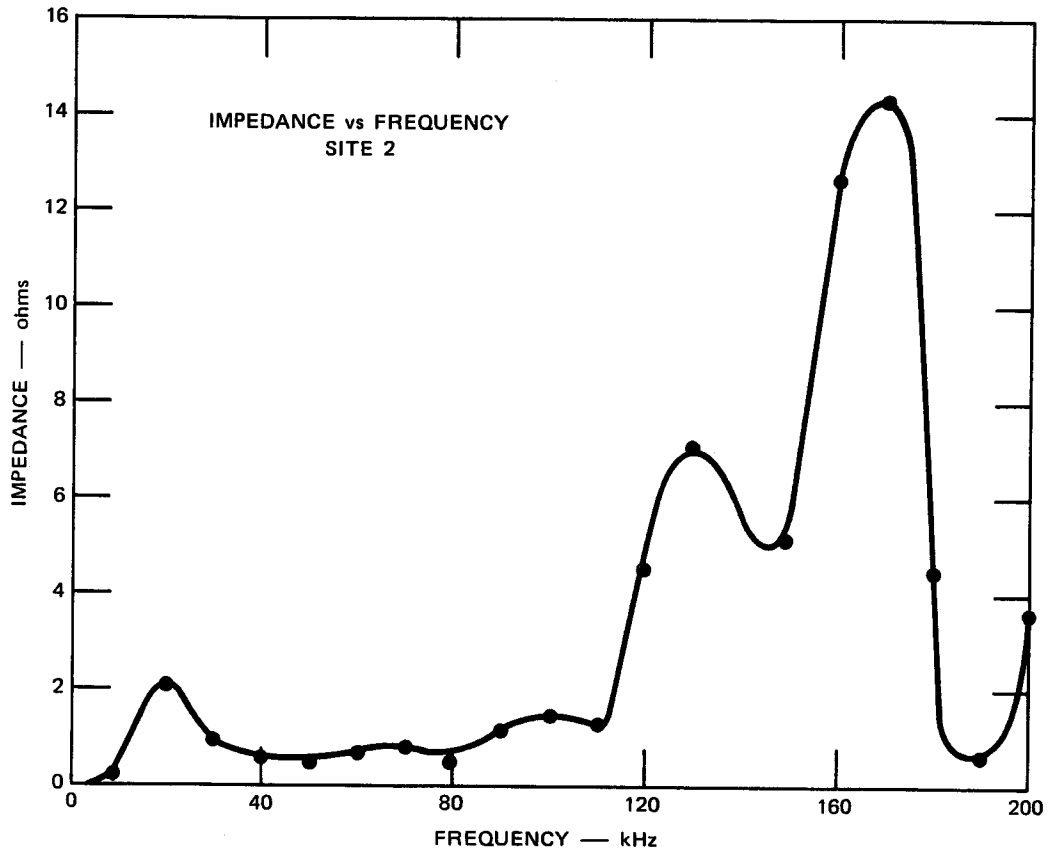


FIGURE 6 IMPEDANCE MAGNITUDE AS A FUNCTION OF FREQUENCY AT SITE 2

receiver without temporal resolution would have produced E- and B-field data that could have produced incorrect and misleading impedance values. The temporal resolution feature of the instrumentation employed in these measurements has been useful in ensuring that impulse-noise data being analyzed are fully understood.

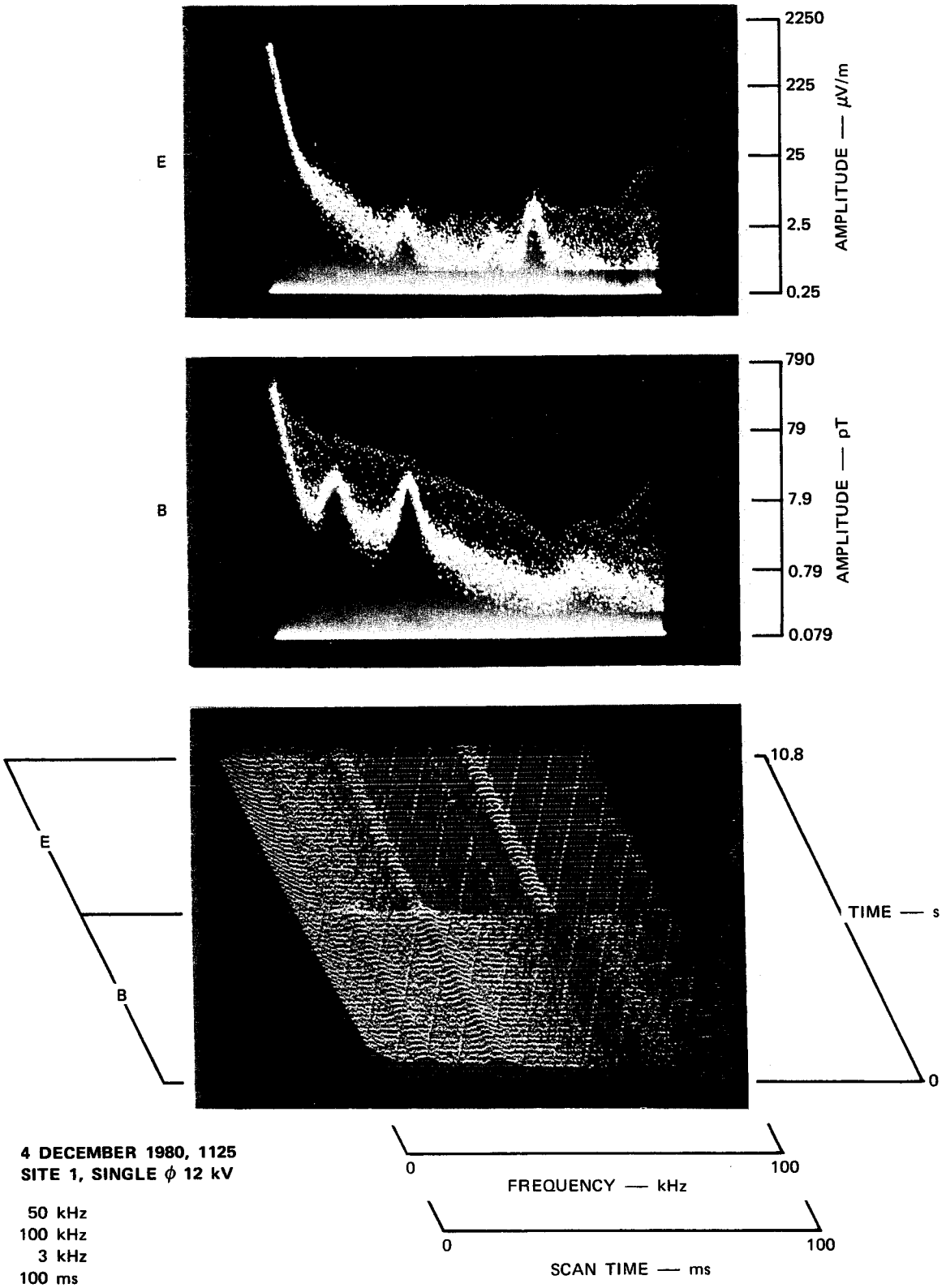


FIGURE 7 E- AND B-FIELD NOISE AT SITE 1 — EARLY EVENING

## VI DISCUSSION

A number of interesting facts were derived from the measurement of radio noise emanating from the selected "noisy" line. The measured noise was impulsive and precisely synchronized with the 60-Hz power-line waveform. This factor suggested that the noise sources were synchronous switching devices operating as loads on the line.

To understand the noise fully, measurements of both the electric- and magnetic-fields associated with the line over broad bands of frequencies were necessary. The dominant E field at the sensor location was vertical, and the dominant B field was horizontal and normal to the overhead wires. The measured field strengths were used to calculate the peak impulse noise voltage and the peak impulse noise current on the overhead wires. The calculated peak values of current and voltage (see Table 1) on the wires were low compared to the voltages and currents on the 60-Hz distribution line; however, the calculated values were significant when viewed as a source of radio frequency interference (RFI). For example, the noise currents and voltages on the line were large when compared to distribution line-power carrier receiver signal levels. The electric and magnetic fields were sufficiently large to interfere seriously with experimental vehicular OMEGA and LORAN-C navigational systems operating along the street. Mobile VHF receiver performance was degraded when operated near the line.

Many published papers and reports contain data from either E-field or B-field measurements with the implication that the field not measured can be related to measured data with the far-field impedance of $120\pi\ \Omega$. However, this procedure is incorrect when the measurements are made within the inductive or quasi-static region around an overhead power line. Most power-line noise measurements are made within this zone, hence both the electric and magnetic fields must be measured independently. The very low values of impedance shown in Figures 4 and 6, when compared

to the far-field value of $120\pi\ \Omega$, demonstrate the large errors involved in single-field measurements of power-line radio noise. The measured values of impedance are similar to direct line impedance measurements reported by others.[13] Both sets of data show that average impedance increases with frequency. At some higher frequency (>30 MHz), the impedance from E- and B-field data will approach the far-field value of $120\pi\ \Omega$. At low frequencies ($< \approx 1$ MHz) the impedance from E- and B-field measurements will approach the impedance of the overhead line with its loads.

The resonant peaks and nulls in noise amplitude shown in Figures 4 and 6 probably were caused by the reactive impedance of nearby transformers, capacitors, and loads. These resonant peaks and nulls will change in frequency and magnitude as such devices are switched on an off. A prior measurement of impulsive noise originating from a known high-power switching device at a time when a power correction capacitor was switched produced a marked change in frequency of a noise peak.[14]

The very large difference in impedance versus frequency for two sites, which were only 150 ft apart (Figures 4 and 6), suggest that transformers, power factor capacitors, and loads establish line impedance levels at noise frequencies rather than the intrinsic impedance of the overhead wires.

The large change in impulse noise properties at Site 1 from midday to early evening indicate that multiple and different noise sources were involved. The evening data in Figure 7 demonstrate the necessity for extreme care in making radio-noise measurements. Measured data can be used to calculate impedance as a function of frequency, but such results will be meaningless because the E and B fields, as shown by the time-domain information, originated from separate sources.

The measured data were described in terms of peak values of E and B fields and their associated peak values of line-noise voltage and current. Additional noise descriptors can be derived from the measured data. For example, average and rms values can be obtained. Amplitude probabilities distributions (APD) of E and B fields or line voltage and current

can be obtained at many discrete frequencies. Amplitude probabilities distributions for the measured data would have produced interesting plots with a discontinuity at the single-valued amplitude of the impulses. Published data on APDs of power-line noise have shown smooth continuous curves associated with random impulse amplitudes rather than with the single-value cases observed.[6,7]

The synchronous impulsive noise carried along and emitted from the selected distribution line was similar to noise found on many other urban, suburban, and rural distribution lines.[9,10] The impulses usually originate from electric-utility customer-load control devices such as SCRs, thyristers, rectifiers, gas-tube switches, and similar devices. Recent measurements have indicated that such devices may be the primary source of distribution-power-line noise.

## REFERENCES


1. E. N. Skomal, Man-Made Radio Noise (Van Nostrand Reinhold Company, New York, NY, 1978).

2. J. R. Herman, Electromagnetic Ambients and Man-Made Noise, Vol. III, Multi-Volume EMC Encyclopedia Series (Don White Consultants, Gainesville, VA, 1979).

3. A. D. Spaulding, "Man-Made Noise: the Problem and Recommended Steps Toward Solution," OT Report 76-85, Office of Telecommunications, U.S. Department of Commerce, Boulder, CO (April 1976).

4. A. D. Spaulding and R. T. Disney, "Man-Made Radio Noise, Part 1: Estimates for Business, Residential, and Rural Areas," OT Report 74-38, Office of Telecommunications, U.S. Department of Commerce, Boulder, CO (June 1974).

5. A. D. Spaulding, R. T. Disney, and A. G. Hubbard, "Man-Made Radio Noise, Part II: Bibliography of Measurement Data, Applications, and Measurement Methods," OT Report 75-63, Office of Telecommunications, U.S. Department of Commerce, Boulder, CO (1975).

6. R. A. Shepard and J. C. Gaddie, "Measurements of the APD and Degradation Caused by Power Line Noise at HF," Final Report, Contract N00039-74-C-0071, SRI Project No. 2997, SRI International, Menlo Park, CA (April 1976).

7. W. R. Lauber, "Amplitude Probability Distribution Measurements at the Apple Grove 7756V Project," IEEE Trans. on Power Apparatus and Systems, Vol. PAS-95, No. 4, pp. 1254-1266 (July/August 1976).

8. D. Middleton, "Statistical-Physical Models of Man-Made Radio Noise," OT Report 74-36, Office of Telecommunications, U.S. Department of Commerce, Boulder, CO (April 1974).

9. R. E. Owen, W. R. Vincent, and W. E. Blair, "Measurement of Impulsive Noise on Electric Distribution Systems," IEEE Trans. on Power Apparatus and Systems, Vol. PAS-99, No. 6, pp. 2433-2438 (November/December 1980).

10. W. R. Vincent, D. Smith, and S. Jauregui, "Temporal and Spectral Properties of Power-Line Noise," Proc. of IEEE International Symposium on EMC, pp. 26-29 (October 1980).

11. F. D. Pullen, "The Calculated Electromagnetic Fields Surrounding Carrier-Bearing Power Line Conductors," IEEE Trans. on Power Apparatus and Systems, Vol. PAS-94, No. 2, pp. 530-538 (March/April 1975).

12. S. Attwood, Electric and Magnetic Field (John Wiley & Sons, New York, NY, 1949).

13. J. R. Nicholson and J. A. Mallach, "RF Impedance of Power Lines and Line Impedance Stabilization Networks in Conducted Interference Measurements," IEEE Trans. on EMC, pp. 84-86 (May 1973).

14. R. E. Owen and M. F. McGranaghan, "Study of Distribution Surge and Harmonic Characteristics," Final Report, Project 1024-1, Electric Power Research Institute, Palo Alto, CA (November 1980).

SRI International

*Technical Memorandum 3564-051783* *17 May 1983*

# DISTRIBUTION-LINE HARMONICS AND NOISE AT EXPORT, PENNSYLVANIA

*By:* W. RAY VINCENT ROBERT L. BOLLEN

*Prepared for:*

ELECTRIC POWER RESEARCH INSTITUTE
3412 HILLVIEW AVENUE
PALO ALTO, CALIFORNIA 94304
Attention: DR. WILLIAM E. BLAIR

EPRI Project RP2017-1

SRI Project 3564

SRI International®
333 Ravenswood Ave. • Menlo Park, CA 94025
(415) 859-6200 • TWX: 910-373-2046 • Telex: 334 486

CONTENTS

ILLUSTRATIONS

# I INTRODUCTION

The Westinghouse Research Laboratory, Pittsburgh, Pennsylvania, has developed an instrument to sense ultrasonic noise that is generated inside a power factor correction capacitor. The instrument was developed to sense minute arcing inside a capacitor that might be associated with capacitor failures. Westinghouse personnel used the instrument to identify two sets of capacitors in the Pittsburgh area that produced ultrasonic noise. The capacitors were located on a 13.8-kV three-phase distribution line in Export, Pennsylvania. The distribution line was owned by Western Pennsylvania Power (WPP).

Under EPRI Project 2017-1, SRI International examined harmonics and noise on the WPP distribution line that might have contributed to reduced capacitor life. SRI also searched for radio noise that capacitor failure mechanisms might produce. An instrumentation van, used on the EPRI Project 2017-1 to examine harmonics and noise on distribution and transmission lines, was temporarily diverted to Export, Pennsylvania, to measure radio noise from selected capacitors. The instrumentation van* was equipped with sensors, receivers, and data analysis equipment to measure, analyze, and define unusual types of signals and radio noise. Arrangements were made by EPRI personnel for Westinghouse and SRI teams to operate their respective equipment over the same period so that the ultrasonic and radio data could be compared.

This technical memorandum describes the results of the SRI measurements on the Export Distribution Line and at the capacitor locations.

---

*A detailed description of the instrumentation van is given in SRI Technical Memorandum 3564-092981, dated September 1981.

## II TEST OBJECTIVES

The objectives of measurements on the 13.8-kV distribution line of Western Pennsylvania Power located in Export, Pennsylvania, were:

(a) To survey the distribution line near the suspected capacitor banks for unusual harmonics and impulsive noise conditions

(b) To examine harmonics and noise at potential sources of unusual or high harmonics or noise

(c) To search for unusual radio noise emanating from capacitor leads and from the distribution line at and near the capacitor location.

# III TEST RESULTS

## A. Measurement Details

Standard electric and magnetic field sensors provided with the instrumentation van were used to measure harmonics and noise on the 13.8-kV distribution line providing electric power to the small town of Export. A map showing a portion of the Export Distribution Line containing the suspected capacitors is shown in Figure 1. Harmonic and noise conditions on the line were surveyed by driving the van slowly along the distribution line. From this survey, a few measurement points were chosen as shown on Figure 1. The van was then parked at each selected measurement point to observe harmonics and noise. At the capacitor locations, additional noise measurements were made at higher frequencies at which gap noise and insulator leakage noise are commonly found. These measurements included a complete survey of signals and noise from 30 Hz to 1000 MHz in an attempt to identify any unusual noise emanating from the capacitors.

Harmonic and noise data observed on the spectral and temporal displays in the instrumentation van were recorded with a Polaroid camera. Typical examples of recorded data are included in this report to illustrate conditions found on the distribution line.

Filters were incorporated into all sensors to deemphasize the amplitude of 60-Hz signals and low-frequency harmonics. These filters were necessary to obtain sufficient instrumentation system dynamic range to view 60-Hz signals and all harmonics present in the measured circuits simultaneously. The filter attenuation characteristics must be used during scaling of photographic data presented in this report. A description of the probes and sensors is given in the Appendix along with filter attenuation curves and conversion constants necessary to scale the raw data.

**T & D OPERATING MANUAL**
FORM 30-822

(Lincoln Division)

WHITE VALLEY STATION
EXPORT 12 KV

SUBSTATION 24048
CIRCUIT 007300
PEAK LOAD 3600KVA 1/82

| | O.H. | U.G. |
|---|---|---|
| 3Ø | 6.2 mi. | 0.1 mi. |
| 2Ø | 4.4 mi. | 0 mi. |
| 1Ø | 20.1 mi. | 2.5 mi. |

TOTAL CUSTOMERS 1620

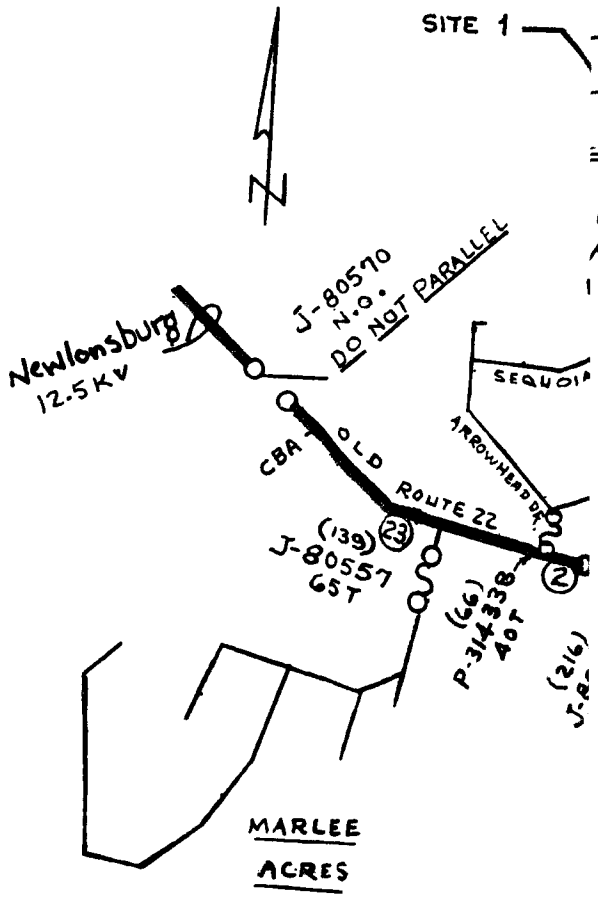


POLE NUMBERS SHOWN ON OLD ITALY ROAD ARE WM. PENN CATV ANTENNA & CRITICAL AMPLIFIER LOCATIONS. GIVE PREFERENTIAL TREATMENT.

1. J.M. HALL & J.M. HALL JR. INC. (120/
2. PENN POWER PRODUCTS (240V)
3. Univ. Welding & Metals Inc. (
4. Extrusion Tool & Die Co. (24
5. WOLFE Funeral Home (240 V.
6. EXPORT V.F.D. (240V.)
7. Watson's Garage (240 V.)
8. SOUTHWEST NATIONAL BANK (120/20
9. Duff's Tire Service (240 V.)
10. Export Metals Co. (240 V.)
11. Geo's Body Shop (240 V.)
12.
13. Export Tire (240 V.)
14. Franklin Estates Sew. (240 V
15. Forbes Trail Auto Parts (240
16.
17. Westmoreland Country Club (2
18. " " " (
19. " " " (
20. HILLS CHURCH TOOL & DIE CO. (120/
21. Banks Engineering Co. (120/2
22. THE HUB DEPT. STORE (120/240V.)
23. D'APPOLONIA CONSULTING ENGR'S

15155
T.P.

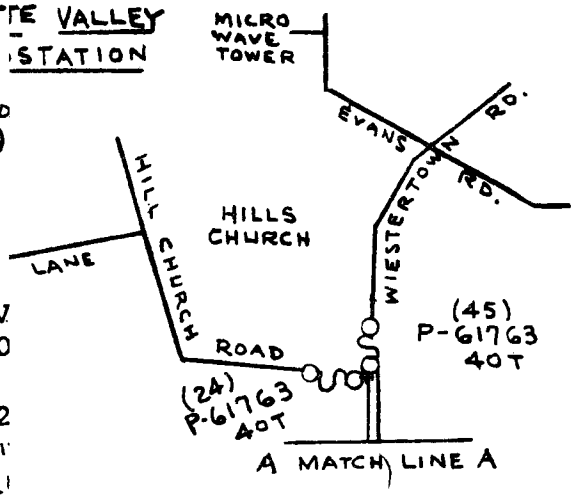


FIGURE 1

## B. General Observations

During the general survey several specific harmonic and noise effects were observed. A very strong 9th voltage and current harmonic was found on the distribution line in the vicinity of the capacitor banks. The 9th harmonic became noticable about 0.5 miles from each capacitor, gradually increased in amplitude as the capacitor bank was approached, reached maximum amplitude about 0.25 miles from each capacitor bank, and remained approximately constant in voltage and current amplitude between the capacitor banks. About midway between the capacitor banks a tee in the line provided power to several houses and two small commercial facilities. The 9th current harmonic remained constant along this tee for about 0.25 miles and then decreased to a low level. The 9th voltage harmonic remained high along the tee until the line reached the Universal Welding building. Strong current transients were observed on the tee. No voltage transients were observed on the tee.

## C. Results From Site 1

Results from the general survey suggested that a measurement location near the junction of the tee providing power to Universal Welding and the main line would be useful. Site 1 was located along the tee about 100 ft from the junction with the main line. Electric- and magnetic-field measurements of harmonics from 0-to-1.0-kHz are shown in Figure 2. The 9th was the dominant E-field harmonic. Additional odd harmonics were found in the data, but they were all lower in amplitude than the 9th. The dominant B-field harmonic was also the 9th, which was only about 12 dB below the 60-Hz current. Additional harmonic structure was also found in the B-field data that was not present in the E-field data. For example, a component is shown in the B-field data at about 30 Hz. The frequency range of the analyzer was decreased to examine the unexpected 30-Hz component closely as shown in Figure 3. The B-field data show significant components at 30, 54, 90, 120, 150, 155, 180, 210, 200, and 240 Hz. The E-field data show only a strong 3rd harmonic and weak 2nd and 4th harmonics. The strong current subharmonic at 30 Hz and its related higher frequency components suggest that a significant load existed on the line with a

$E_z$

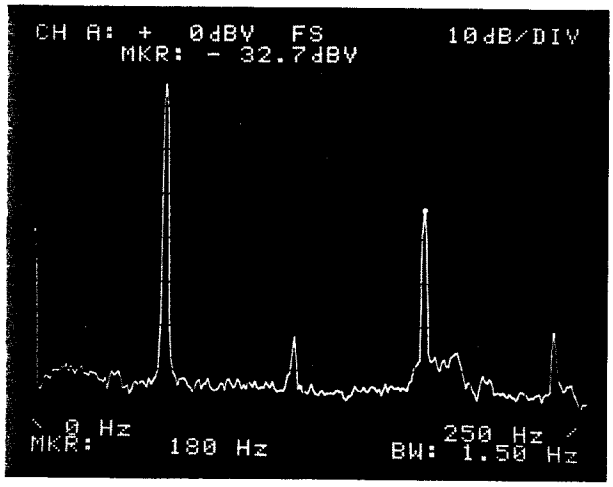


$B_x$

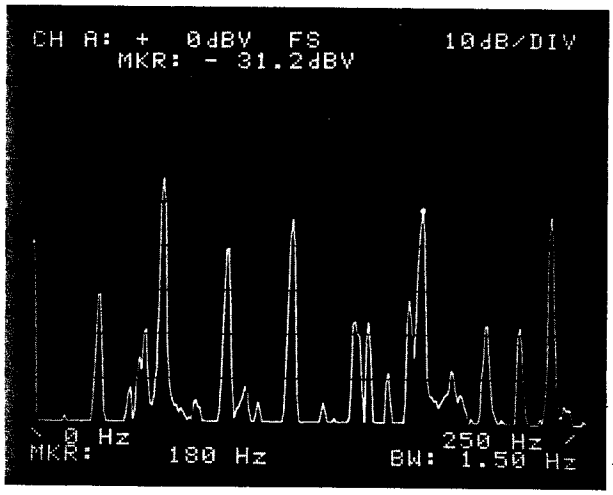


**1657, 9-15-82**
**WPP, WV, E, SITE 2**
**$E_z$, + 50**
**$B_x$, + 40**
**(Amplitude scale must be corrected using Figure A-1 for the E field and Figure A-2 for the B field)**

FIGURE 3 VOLTAGE AND CURRENT HARMONICS, 0 TO 250 Hz, SITE 2

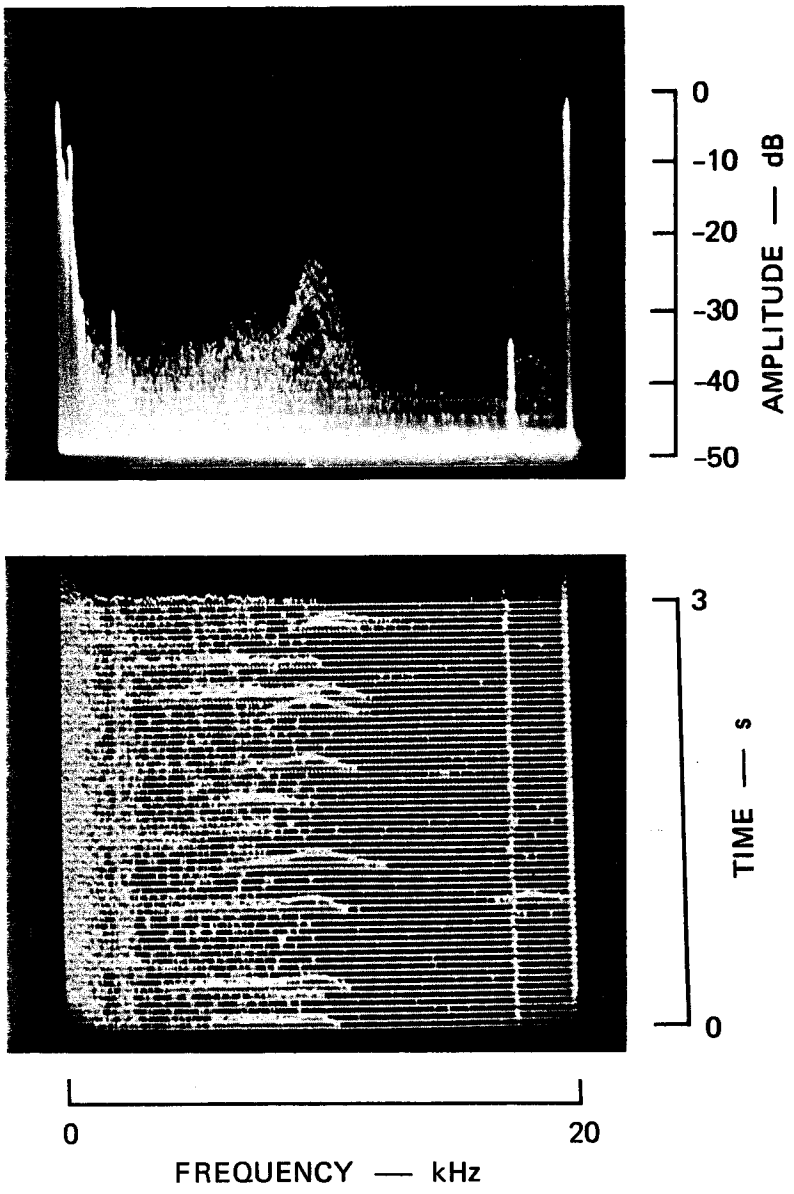


**1721, 9-15-82**
**WPP, WV, E, SITE 2**
**$B_X$, + 30, - 20, + 10**
**0, 20, T20, X 1**
**(Amplitude scale must be corrected using Figure A-2)**

FIGURE 4 CURRENT BURSTS WITH SPECTRAL ENERGY CENTERED AT 10 kHz